Brazilian Journal of Microbiology (2020) 51:467–487
https://doi.org/10.1007/s42770-020-00235-y

BACTERIAL AND FUNGAL PATHOGENESIS - RESEARCH PAPER

Inhibition of quorum sensing–associated virulence factors and biofilm formation in *Pseudomonas aeruginosa* PAO1 by *Mycoleptodiscus indicus* PUTY1

Tanveer Ahmed[1] · Subhaswaraj Pattnaik[2] · Mohd Babu Khan[3] · Dinakara Rao Ampasala[3] · Siddhardha Busi[2] · V. Venkateswara Sarma[1]

Received: 18 April 2019 / Accepted: 28 January 2020 / Published online: 21 February 2020

Abstract

Pseudomonas aeruginosa is the second most emerging multidrug-resistant, opportunistic pathogen after *Acinetobacter baumannii* that poses a threat in nursing homes, hospitals, and patients who need devices such as ventilators and blood catheters. Its ability to form quorum sensing–regulated virulence factors and biofilm makes it more resistant to top most therapeutic agents such as carbapenems and next-generation antibiotics. In the current study, we studied the quorum quenching potential of secondary metabolites of *Mycoleptodiscus indicus* PUTY1 strain. In vitro observation showed a mitigation in virulence factors such as rhamnolipids, protease, elastase pyocyanin, exopolysaccharides, and hydrogen cyanide gas. Furthermore, a significant reduction in the motility such as swimming, swarming, twitching, and inhibition in biofilm formation by *Pseudomonas aeruginosa* PAO1 was observed. Results of in vitro studies were further confirmed by in silico studies through docking and molecular dynamic simulation of GC-MS-detected compounds of *Mycoleptodiscus indicus* employing LasR and RhlR proteins. Both in vitro and in silico observations indicate a new alternative approach for combating virulence of *Pseudomonas aeruginosa* by targeting its protein receptors LasR and RhlR.

Keywords Antibiotic resistance · Attenuation · Fungal secondary metabolites · Quorum quenching · Saprophytes

Introduction

Increasing incidents of multi drug resistance among human pathogens poses an alarming threat to human beings throughout the world [1]. Presently, a global concern has emerged as we are passing through a post-antibiotic era where we find a reduced ability to combat microbes [2]. Traditional approaches to overcome microbial infections have not been found to be so effective and hence, targeting the virulence of microbes presents a more pioneering approach. The strategies focused for generation of future antimicrobial agents include those that can improve the efficacy of drugs and thus help reduce the multidrug resistance [3]. Identification of new natural bioactive compounds to manage and mitigate different microbial infections has become a need of the hour. One of the strategies targeted could be the genetic pathways for bacterial control as these pathways are vital for bacterial virulence. Some pathogenic Gram-negative bacteria such as *Pseudomonas aeruginosa*, *Burkholderia cepacia*, and *Serratia marcescens* possess acylated homoserine lactone (AHL)–based quorum sensing (QS) system, which aids in infection process. *Pseudomonas aeruginosa* is ubiquitous in nature and occupies different aquatic and terrestrial habitats. It infects various plants and animals including human beings [4–6] by forming biofilms, which aid in bacterial pathogenesis. Such bacteria are resistant to chemical disinfectants, drugs, and the action of host immune defenses [7, 8]. *P. aeruginosa* PAO1, having a genome size of 6.2Mbp, encodes for approximately 435 one-component systems (OCSs) and 130 two-component systems (TCSs) [9]. TCSs in the *P. aeruginosa*

Responsible Editor: Cristiano Gallina Moreira.

✉ V. Venkateswara Sarma
sarmavv@yahoo.com

[1] Department of Biotechnology, School of Life Sciences, Pondicherry University, Puducherry 605014, India

[2] Department of Microbiology, School of Life Sciences, Pondicherry University, Puducherry 605014, India

[3] Centre for Bioinformatics, School of Life Sciences, Pondicherry University, Puducherry 605014, India

act as crucial sensory systems that allow the bacterial adaptation in the adverse environment as well as in the host [10]. TCSs play a crucial role in the regulation of gene expression in response to external stimuli, which in turn regulate the production of virulence factors and biofilm formation. Among the known TCSs, the *GacS/GacA* works as a super regulator of the QS network because it controls the AHL system by inactivating the RsmA protein. This results in a negative regulation of the synthesis of 3-oxo-C12-HSL and C4-HSL and the signaling molecule of las and rhl system respectively. Thus, *GacS/GacA* TCS is directly involved in the synthesis of various types of virulence factors and biofilm formation [11]. *P. aeruginosa* has evolved a complex QS system for bacterial virulence [12]. Therefore, the infection by *P. aeruginosa* can be controlled if the QS-regulated pathways especially lasI/lasR and rhlI/rhlR systems are targeted [13]. Natural biologically active compounds obtained from various plants possess important therapeutic properties, which can be utilized to make next-generation antimicrobial agents that will help to overcome antibiotic resistance. Many plant-derived phytoconstituents such as baicalein from *Scutellaria baicalensis*, zingerone and 6-gingerol from *Zingiber officinale*, and naringenin from *Combretum albiflorum* have been found to significantly alleviate the QS-regulated virulence factors in *P. aeruginosa* [14–16]. The development of antimicrobial agents to inhibit quorum sensing from fungal sources is less explored and hence is a promising area. Our study aimed to disrupt the process of QS regulated virulence factors in *P. aeruginosa* by using a saprophytic leaf litter degrading fungus *Mycoleptodiscus indicus* PUTY1.

Materials and methods

Chemicals and solvents

The chemicals used in the present research such as azocasein and elastin Congo red (ECR) were purchased from Sigma Aldrich, USA. Other chemicals like crystal violet, acridine orange, trichloro acetic acid (TCA), sodium chloride (NaCl), Tris-HCl, and nutrient media such as Tryptone Soy Broth (TSB), Luria Bertani (LB) broth, bacteriological peptone, and LB agar were procured from HiMedia Lab. Pvt. Ltd. (Mumbai, India), and solvent such as ethyl acetate purchased from Avra synthesis Pvt. Ltd. (Hyderabad, India).

Isolation of fungal isolates, media, and storage

Dead and decomposing leaf litter samples of *Tridax procumbens* were collected from the main campus of Pondicherry University (12° 00′ 57″ N, 79° 51′ 30.1″ E) (Pondicherry, India). A total of 45 fungal isolates were primarily isolated from leaf litter samples through a modified particle filtration technique [17]. Briefly, the leaf litter samples were first cleaned carefully with the tap water followed by sterile distilled water and were dried at room temperature. One gram of dried leaves was ground in a blender and diluted with 100 mL sterile distilled water to form a particle suspension. From this, 500 μL was poured in the plates using pour plate method. The colonies propping up from the PDA plates were subcultured to get axenic cultures. All the pure fungal isolates were preserved at − 80 °C in 15% glycerol solution in cryovials for further analysis.

Extraction of fungal crude extracts and sample preparation

Fungal isolates were aseptically grown in 1000-mL conical flasks containing potato dextrose broth (PDB) by incubating under static conditions at 25 °C ± 2, after inoculating with freshly grown fungal mycelial bits. After 2 weeks of growth, the mycelial mat was separated from the broth by using three layers of muslin cloth and broth was centrifuged at 10,000 rpm for 20 min to remove any fungal spores and tiny mycelial bits settling as pellet. The resulting filtrate was extracted twice with equal volumes of ethyl acetate and kept on a shaker (200 rpm) for 24–48 h for separation of secondary metabolites. Both aqueous and organic phases were separated through glass separatory funnel and organic phase of ethyl acetate was concentrated by rotary vacuum evaporator (Buchi, India) to collect crude extracts [18]. Fungal crude extracts were dissolved in DMSO for preliminary screening and for further in vitro analysis in required concentrations.

Screening of fungal crude extracts

Fungal isolates were subjected to preliminary screening for their antiquorum sensing potential against an ideal model strain *Chromobacterium violaceum* (MTCC 2656) and *P. aeruginosa* (MTCC 2453), following agar well diffusion method as per Oliveira et al. (2016) with minor modification. In brief, 10 mL of molten soft agar (Tryptone 10 g/L, NaCl 5 g/L, agar 6.5 g/L), seeded with 1% overnight culture of either *P. aeruginosa* or *C. violaceum*, was poured separately onto the fresh LB agar medium and was allowed to solidify. Two wells with a diameter of 8 mm were carefully made and two different doses of fungal crude extracts (250 and 500 μg/mL) were loaded into each well and the plates were incubated at 37 °C for 24 h [19].

Identification of potential fungal isolate through sequencing

Based on the results of initial screening for antiquorum sensing potential of fungal crude extracts, one fungal isolate PUTY1 was chosen for further studies and was selected for

molecular identification. The internal transcribed spacer (ITS) region of the fungal isolate PUTY1 was amplified using specific primers ITS1 (5′-TCCGTAGGTGAACCTGCGG-3′) and ITS4 (5′- TCCTCCGCTTATTGATATGC-3′). The amplified PCR products were subjected to gel electrophoresis to check the purity of amplicons and specific band was purified and sequenced. The sequences obtained were compared for homology using BLASTN (NCBI) database [20]. The ITS sequence was subjected to multiple sequence alignment followed by phylogenetic analysis for molecular identification.

Phylogenetic analyses

Phylogenetic analysis was performed under maximum likelihood (ML), maximum parsimony (MP), and Bayesian (BYPP) criteria. Parsimony analysis was carried with the heuristic search option in PAUP (Phylogenetic Analysis Using Parsimony) v.4. Bayesian analysis was conducted with MrBayes v. 3.1.2 [21] to evaluate Bayesian posterior probabilities (BYPP) [22] by Markov Chain Monte Carlo sampling (BMCMC). GTR + I + G was used in the command. Six simultaneous Markov chains were run for 5,000,000 generations and trees were sampled every 1000th generation. First 20% of generated trees were rejected and remaining 80% of trees were used to calculate posterior probabilities of the majority rule consensus tree. BYPP greater than 0.60 are given above each node. Maximum likelihood trees were generated using the RAxML-HPC2 on XSEDE (8.2.8) [23] in the CIPRES Science Gateway platform [24] using GTR + I + G model of evolution. Phylograms were visualized with FigTree v1.4.0 program and reorganized in Microsoft power point (2007) and Adobe Illustrator® CS5 (version 15.0.0, Adobe®, San Jose, CA).

Determination of minimum inhibitory concentration

The minimum inhibitory concentration (MIC) of *M. indicus* extract against *P. aeruginosa* was determined using a broth microdilution method with bacterial concentration of 1×10^5 CFU/mL in LB broth following the guideline of Clinical and Laboratory Standards Institute [25].

Violacein inhibition activity

In this test, the overnight culture of *C. violaceum* (MTCC 2656) was inoculated into freshly prepared LB medium supplemented with and without *M. indicus* crude extract and incubated at 37 °C for 24 h. After incubation, the cultures were centrifuged at 13,000 rpm for 10 min for the precipitation of insoluble violacein. The pellets were resuspended in DMSO and the suspension was vigorously vortexed followed by recentrifugation at 13,000 rpm for 10 min. The absorbance of the supernatant was measured at 585 nm. The *C. violaceum* culture without PUTY1 extract acted as control [25].

Growth curve analysis

The effect of sub-MIC concentration of PUTY1 extract on the growth and cell proliferation of *P. aeruginosa* PAO1 was monitored at 600 nm for 24 h at every 1-h interval by using spectrophotometer [26].

Effect of *M. indicus* extract on QS-regulated virulence factors of *P. aeruginosa*

Pyocyanin inhibition activity

To measure the inhibition of pyocyanin pigment, the bacterium was inoculated with and without the sub-MIC concentration of *M. indicus* extract, and after overnight incubation at 37 °C, pyocyanin pigment was extracted from cell-free supernatant using chloroform in the ratio of 3:2 and then re-extracted using 0.2 M HCl to obtain a pink-colored solution. The intensity of the solution was recorded at 520 nm [27].

LasA protease activity

Azocasein degrading activity was determined by adding overnight grown culture supernatant of *P. aeruginosa* (with treated or without treated) to 1 mL of 0.3% azocasein in 0.05 M Tris–HCl (pH 7.5) and incubated at 37 °C for 15 min. Then, 10% TCA was added to stop the reaction followed by centrifugation at 10,000 rpm for 5 min to get clear supernatant and absorbance was measured at 440 nm [28].

LasB elastase activity

This activity was measured following the method of Das et al. [28]. In brief, 100 μL of PUTY1 treated cell-free culture supernatant of *P. aeruginosa* was added to 900 μL of ECR buffer (100 mM Tris, 1 mM CaCl2, pH 7.5) containing 20 mg of elastin Congo red and was incubated at 37 °C for 3 h under appropriate shaking conditions. The reaction was stopped by using 1 mL of 0.7 M sodium phosphate buffer (pH 6.0) and the tubes were kept in cold water bath. The insoluble ECR was pelleted by centrifugation at 10,000 rpm for 10 min and the OD was recorded at 495 nm [28].

Motility inhibition assay

Swimming and swarming inhibition assays

The method mentioned by Packiavathy et al. [29] was followed for swimming and swarming motility assays; PUTY1

extract treated overnight culture of *P. aeruginosa* was point inoculated onto the center of specific swimming agar medium (tryptone 10 g/L, NaCl 5 g/L, agar 3 g/L). In the case of swarming assay, overnight culture of *P. aeruginosa* was point inoculated at the center of swarming agar medium (10 g/L peptone, 5 g/L NaCl, 5 g/L agar, and 5 g/L filter sterilized glucose) having sub-MIC concentration of PUTY1 extract (750 μg/mL). All the plates were incubated at 37 °C for 24 h [29].

Twitching motility assay

LB agar plates (10 g/L Bacto agar) with and without treatment with sub-MIC concentration of PUTY1 extracts were prepared for twitching motility assay. Overnight cultures of *P. aeruginosa* were stabbed with a sterile toothpick through the LB agar layer to the bottom of the petri dish and then incubated at 37 °C for 48 h. The bacterial adherence to the bottom of the petri plate was examined carefully after removing the agar and staining the adhered cells with crystal violet (0.1%, *w/v*) solution. The petri plates were then washed gently with tap water to remove non-adherent cells before staining. The diameter of zone was measured [30].

Congo red agar method (qualitative biofilm production assay)

Briefly, sterilized aqueous solution of Congo red dye (0.8 g/L) was added to pre-cooled sterile medium containing brain heart infusion agar (BHI) (37 g/L), sucrose (50 g/L), and agar (10 g/L) supplemented with PUTY1 extract (750 μg/mL); fresh culture of *P. aeruginosa* was streaked on the Congo red agar (CRA) plates. The plates were incubated at 37 °C for 48 h and the color of the colonies formed was observed. Plate without *M. indicus* PUTY1 extract worked as control [31].

Rhamnolipid inhibition assay

Briefly, *P. aeruginosa* was grown in the presence and absence of PUTY1 fungal extract at 37 °C for 18 h in LB medium. Cultures were then centrifuged at 10,000 rpm for 5 min. The supernatant was added with equal portion of ethyl acetate and vortexed rigorously to yield rhamnolipid containing layer. The rhamnolipid containing organic phase was dissolved in 99% chloroform and freshly prepared methylene blue solution (1.4% (*w/v*), pH 8.6 ± 0.2) in a 10:1 ratio and the resultant was vortexed. The chloroform phase was transferred to 0.2 N HCl solution and was vortexed again. Finally, OD of the upper acid phase containing methylene blue complex was measured at 638 nm [32].

EPS inhibition assay

The EPS production in *P. aeruginosa* treated with *M. indicus* extract was performed as per Gupta et al. [33] with few modifications. In brief, overnight culture of *P. aeruginosa* was grown with and without PUTY1 extract at 37 °C for 18 h followed by centrifugation at 10,000 rpm, for 15 min and the collected pellets were resuspended in buffer (10 mM KPO_4, pH 7, 5 mM NaCl, 2.5 mM $MgSO_4$) and then recentrifuged at 10,000 rpm for 30 min. The supernatant containing displaced EPS was mixed with three volumes of chilled absolute ethanol and after overnight incubation at 4 °C, the precipitated EPS was added to a mixture of cold phenol (5%) and conc. H_2SO_4 and the absorbance was determined spectrophotometrically at 490 nm [33].

Effect of *M. indicus* extract on alginate production

Culture of *P. aeruginosa* was grown overnight with and without *M. indicus* extract. In brief, 500 μL of 1 M NaCl was mixed to 500 μL of overnight bacterial culture and vortexed followed by centrifugation at 10,000 rpm for 20 min. Then 500 μL of cetylpyridinium chloride was added to the supernatant, mixed rigorously, and recentrifuged at 10,000 rpm for 10 min. The pellet obtained was resuspended in 500 μL of cold isopropanol for 10 min. This mixture was then recentrifuged at 10,000 rpm for 10 min, and finally, the obtained pellet was resuspended in 500 μL of 1 M NaCl for overnight and alginate was quantified by carbazole assay [34, 35].

LasA staphylolytic activity

The LasA staphylolytic protease activity of *P. aeruginosa* was measured by determining its ability to lyse-boiled culture of *Staphylococcus aureus* on treatment with PUTY1 extract. In brief, 30 mL overnight culture of *S. aureus* was boiled for 10–12 min and then centrifuged for 10 min at 13,000 rpm and the resultant pellet was resuspended in 10 mM Na_2PO_4 (pH 4.5). A 100-μL aliquot of *P. aeruginosa* test supernatant with the crude extract was added to 900 μL of the *S. aureus* suspension The OD of the mixture was recorded at every 15-min interval up to 2 h at 600 nm [36]. The percentage of inhibition was calculated as follows:

Staphylolytic activity (%) = (change in OD_{600}/h in control − change in OD_{600}/h in treated sample) / (change in OD_{600}/h in control) × 100

Biomass assay with crystal violet

The biofilm formation activity of *P. aeruginosa* after treatment with *M. indicus* extract was quantified by following the method of Luciardi et al. [37] with slight modification. The

biofilms formed after 24 h of incubation were stained with an aqueous solution of crystal violet (0.1% *w*/*v*) for 20 min followed by washing with water. The biofilms that remained fixed to the polystyrene were genially washed with PBS thrice. The stain bound to biofilm was then dissolved by adding 95% ethanol and the OD was measured at 595 nm [37].

Determination of cell surface hydrophobicity

For determination of cell surface hydrophobicity (CSH), overnight culture of *P. aeruginosa* containing with and without *M. indicus* extract was grown for 24 h and centrifuged at 12,000 rpm for 2 min. The pellets were washed gently and homogenized in PUM buffer (22.2 g potassium phosphate trihydrate, 7.26 g monobasic potassium phosphate, 1.8 g urea, and 0.2 g magnesium sulfate heptahydrate/l (pH 7.1). A 100-μL suspension was taken out to measure the initial cell density (ICD). 400 μL of toluene was added in the rest of suspension and vortexed. The aqueous layer was collected, and the final cell density (FCD) was measured [38]. The percentage of hydrophobicity was calculated as follows:

$$\text{Hydrophobicity}\ (\%) = (\text{ICD}-\text{FCD})/\text{ICD} \times 100.$$

Inhibition of hydrogen cyanide production

Hydrogen cyanide (HCN) production was observed by change in the color of Whatman No. 1 filter paper. Briefly *P. aeruginosa* PAO1 was streaked on to nutrient agar medium supplemented with 4.4 g/L of glycine and with and without *M. indicus* extract. Filter papers were saturated in a solution (2% sodium carbonate and 0.5% picric acid) and kept in the upper lid of petri dishes. Plates were sealed with parafilm appropriately to avoid the gas from escaping. Plates were incubated at 28 °C for 4 days. One plate without inoculation of bacterium was considered as negative control and one plate without the fungal extract was considered as positive control. Production of HCN gas turns yellow filter papers into cream, light brown, dark brown, and finally reddish-brown color [39].

Microscopic observation of adherence of bacterial cell on coverslip

Fresh culture of *P. aeruginosa* was added in the sterilized LB broth with and without the supplementation of *M. indicus* extract and a sterilized coverslip and was incubated at 37 °C for 16 h. After incubation, the coverslips were washed gently with PBS to remove unattached cells. Then the coverslips adhering bacterial cells were stained with 0.4% crystal violet solution and observed under differential interference contrast (DIC) microscope in × 100 magnification (Kalia et al., 2015). In the case of fluorescence microscopic observations, the bacterial biofilms adhering to the coverslips were stained with 0.01% acridine orange for 15–20 min in dark and allowed to air dry. Adhered cells were fixed by using 2.5% glutaraldehyde. Then the coverslips were observed under fluorescence microscope at × 40 magnification [28].

GC-MS analysis of *M. indicus* extract

GC-MS analysis of the *M. indicus* crude extract was executed to detect the presence of bioactive components. GC-MS analysis was accomplished at sophisticated instrumentation facility (Vellore Institute of Technology, 632 014, TN, India).

In silico studies

Modeling and structure validation

In *P. aeruginosa*, QS is regulated by two critical circuits, i.e., las and rhl, which activate the expression of QS-responsive gene. Upon binding to their respective autoinducers *N*-(3-oxododecanoyl)-homoserine lactone (OdDHL) and *N*-butyrylhomoserine lactone (BHL), the receptor proteins LasR and RhlR get activated and this inducer-receptor complex further binds to the conserved las-rhl boxes residing in the promoters of target genes and regulate the target gene expression. In the present study, to check the binding affinity of the compounds present in the fungal secondary metabolites, the structure of LasR protein was retrieved from the PDB database (PDB ID: 2uv0, Chain H). Due to unavailability of crystal structure of RhlR protein in PDB database, its amino acid sequence was retrieved from the UniProt database (ID: P54292.1) and submitted to the online ROBETTA server for the prediction of three-dimensional structure. Finally, the obtained 3D models were confirmed using online RAMPAGE server (http://mordred.bioc.cam.ac.uk/~rapper/rampage.php) and qualities of the predictive models were refined by Verify 3D structure evaluation server (http://nihserver.mbi.ucla.edu/Verify3D/), and the best model was preferred for docking studies [40]. The ligand binding site of both the proteins was predicted via Coach Webserver (https://zhanglab.ccmb.med.umich.edu/COACH/). The ligands used for docking studies include the natural ligand, positive control, and six other ligands for LasR and RhlR. The 3D structures of all these ligands have been prepared by using the Marvin Sketch software (www.marvinsketch.com).

Molecular docking studies

Glide version 11.5 in Schrodinger Maestro version 10.6 (Schrodinger LLC, New York) has been applied for molecular docking studies to prepare LasR & RhlR proteins, whose bond

orders were assigned including the addition of hydrogen and all the water molecules were removed. In this way, proteins were improved by using OPLS force field. Glide version 11.5 in Schrödinger maestro suite was used for grid generation. Docking grid was generated for the proteins LasR and RhlR by using the residues present in their active sites, Tyr-56, Trp-60, Asp-73, Thr-75, Ser-129, and Trp-68 respectively where their respective natural autoinducers interacted. All possible states of ligands at neutral pH were generated in ionized and tautomeric forms with the help of LigPrep module 2.5 in Schrödinger maestro version 9.2 and were optimized by using OPLS force field. Finally, the proteins (LasR and RhlR) and ligands were docked by using molecular docking suit Glide, version 11.5 in Schrödinger maestro suite in extra precision (XP) mode. The 0.8 scale factor and less than 0.15 partial atomic charge was applied to the atoms of both proteins for van der Waals radii. The number of poses generated for each ligand was set criteria up to 10,000 and out of them, 10 best poses per ligand were taken into the consideration. The best docked complex from each of the ligand docking calculation was chosen based on glide score function value and interaction of the relative docked complexes were taken up for further studies [28].

Molecular dynamics simulations

The behavior of protein-ligand (LasR-ligand and Rhlr-ligand) complexes was studied with the help of molecular dynamics (MD) simulation by using the program GROMACS 5.1.2. Initially, the topology files for docked LasR-ligand complexes of the representative protein (PDB ID: 1VU0, Chain H) with the natural ligand, positive control, and other docked compounds were created by using pdb2gmx. Both generated protein structures were processed further on "What If server" [41]. Ligand topology was generated by using the PRODRG server [42], by selecting the chirality charges and no energy minimization for both receptors. Later, energy minimization steps for both the receptor-ligand complexes were carried out to relax the internal constraint of the complexes by using steepest descent algorithm method on GROMOS96 43a1 force field parameter. Further, proteins were solvated by SPC216 with Spce-ignh water model in the triclinic box size of 1.0-nm distance. The complex having the best dock pose with binding score was chosen as a starting structure for MD simulations. The bond angles and geometry of the water molecules were constrained with LINCS [43] and SETTLE [44] algorithm respectively. The van der Waals and electrostatic long-range interactions were applied by using fast particle mesh Ewald (PME) electrostatics [45]. Additional Parrinello-Rahman [46] method was used to regulate the pressure while modified weak coupling Bearsden thermostat and V-rescale algorithm were used to regulate the temperature of the system. Both NVT and NPT were accomplished for 100 ps and monitored for their equilibration status. Finally, the system was subjected to 30 ns of production MD simulation run with a time frame of 2 fs.

Statistical analysis and percentage inhibition calculation

All the tests were performed in triplicates. The outcomes were shown as mean ± standard deviation (SD). To determine the significance, one-way (ANOVA) followed by Tukey's Q test were carried out between the different test groups of different sub-MIC values by using the SPSS software version 20.0, at 5% level of significance. Values (*) are significantly different from 250 μg/mL at $p < 0.05$.

Percentage inhibition was calculated for various assays as follows:

$$\text{Inhibition}\ (\%) = \left[\left(A_{\cdot\text{Control}} - A_{\cdot\text{Sample}}\right)/A_{\cdot\text{Control}}\right] \times 100$$

where $A_{\cdot\text{Control}}$ is the absorbance of the control and $A_{\cdot\text{Sample}}$ is the absorbance of treated sample.

Results

Antiquorum sensing activity of *M. indicus* extracts

Based on the screening results of 45 fungal isolates, *M. indicus* was shortlisted as its extract exhibited highest quorum quenching potential against *C. violaceum* and *P. aeruginosa* with 25-mm and 20-mm zones of inhibition respectively at a dose of 250 μg/mL. Therefore, *M. indicus* extract was preferred for further studies against *P. aeruginosa*.

Molecular identification of PUTY1 fungal strain

The BLAST search analyses of our sequence at NCBI GenBank revealed that our selected fungal isolate PUTY1 showed 100% homology with *Mycoleptodiscus indicus*. The ITS gene dataset comprised 17 taxa including our newly sequenced taxon along with *Pyricularia urashimae* as outgroup from Magnaporthaceae. The trees generated under ML, MP, and BYPP analyses were similar in overall topologies. Phylogeny inferred from ML, MP, and BYPP analyses depicts that our taxon nested with *Mycoleptodiscus indicus* with moderate bootstrap support (Fig. 1). Our sequence generated was submitted to the NCBI GenBank with the name *Mycoleptodiscus indicus* PUTY1 with KY550710 as its accession number.

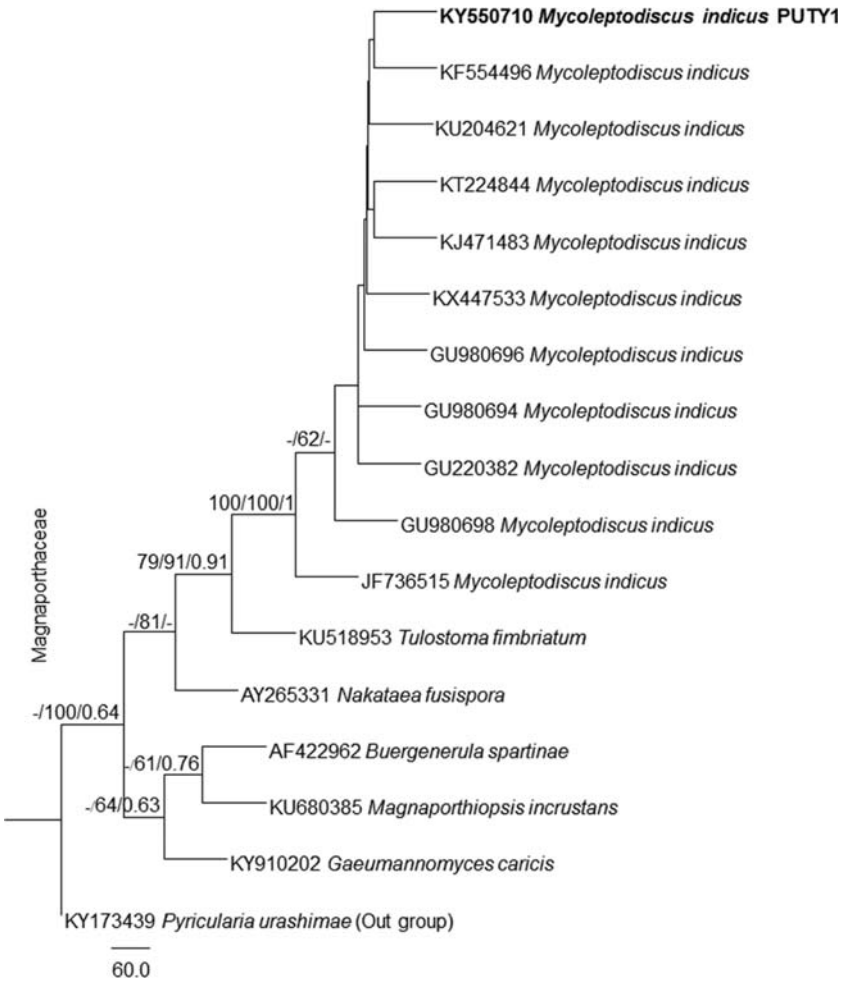

Fig. 1 Paup tree based on analysis of ITS partial sequence data. Bootstrap support values for ML and MP higher than 60% and BYPP greater than 0.60 are given above each branch respectively. The fungal isolate of present study is in bold (*Mycoleptodiscus indicus* PUTY1). The tree is rooted to *Pyricularia urashimae*

Determination of MIC and sub-MIC and analysis of growth curve

The effect of various concentrations of *M. indicus* PUTY1 extract on the growth of *P. aeruginosa* was investigated. Turbidity was not observed at and beyond the concentration of 1000 μg/mL. Therefore, 1000 μg/mL was considered as MIC and following sub-MIC concentration, i.e., 250, 500, and 750 μg/mL were selected for our studies. Growth curve analysis was observed when *P. aeruginosa* was treated with *M. indicus* extract. A significant sigmoid growth curve was observed same as in control with slow growth rate at 750 μg/mL suggesting that it is not perturbing the viability of the cells (Fig. 2(A)).

Violacein pigment inhibition assay

M. indicus extract showed a significant reduction in violacein production by *C. violaceum* in comparison with untreated control with 48.16 ± 1.23, 68.01 ± 1.32, and 84.15 ± 0.99% of reduction at 250-, 500-, and 750-μg/mL concentrations respectively (Fig. 2(B)).

M. indicus extract effect on virulence factors

Effect on pyocyanin, LasA protease, and LasB elastase production

A significant decrease in the pyocyanin production was observed when it was treated with *M. indicus* extract as compared with untreated control with 59.68 ± 1.58, 71.47 ± 2.03, and 75.22 ± 2.31% decrease at 250, 500, and 750 μg/mL sub-MIC respectively (Fig. 2(B)). The effect of *M. indicus* extract on azocasein degrading potential of *P. aeruginosa* was investigated. A marked reduction in protease activity as 49.98 ± 1.94, 64.56 ± 1.24, and 70.09 ± 3.68% at 250-, 500-, and 750-μg/mL concentrations respectively was observed when treated with PUTY1with respect to the untreated control (Fig. 2(B)). The expression of elastase enzyme is very crucial for *P. aeruginosa* as it plays an important role in infecting the patients. In this experiment, a clear reduction in elastolytic activity of *P. aeruginosa* was observed when treated with sub-MIC doses of *M. indicus* extract as shown in the Fig. 2(B) with an inhibition of 43.68 ± 3.2, 63.38 ± 1.76, and 75.57 ± 3.11% at 250, 500, and 750 μg/mL concentrations respectively (Fig. 2(B)).

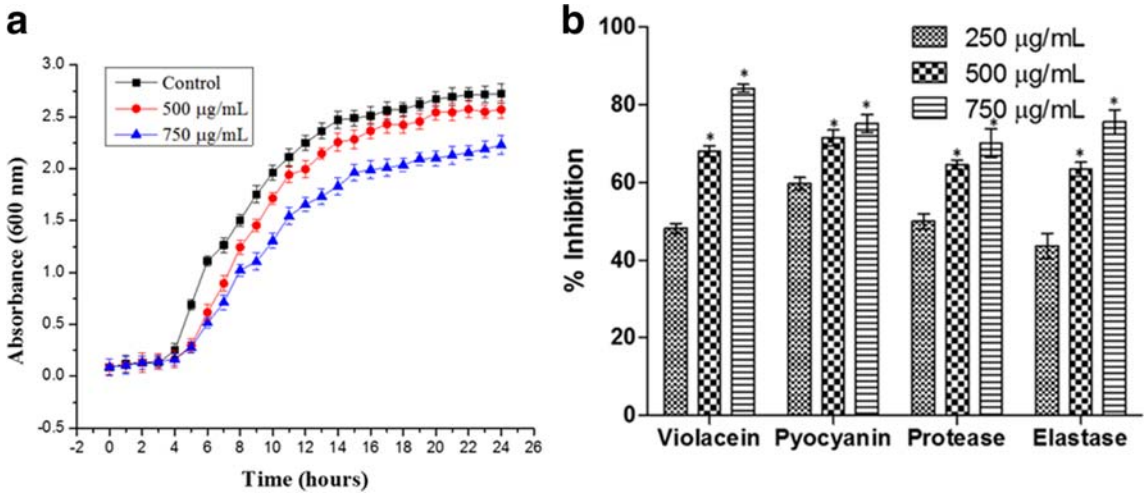

Fig. 2 (A) The effect of *M. indicus* extract at a dose of 500 µg/mL and 750 µg/mL on the growth of *P. aeruginosa* in comparison control. (B) Effect of *M. indicus* extract at concentrations of 250, 500, and 750 µg/mL on violacein production in *C. violaceum* and pyocyanin, protease, and elastase production in *P. aeruginosa*

Inhibition in motility

When treated with *M. indicus* extract, an inhibition in motility of *P. aeruginosa* such as swimming, swarming, and twitching was observed with an inhibition of 94.09 ± 1.71, 86.86 ± 1.24, and 97.32 ± 1.64% respectively at 750-µg/mL concentration with respect to the untreated control (Fig. 3).

Effect on EPS production as evidenced from Congo red agar method

P. aeruginosa treated with *M. indicus* extract at 750 µg/mL showed whitish colonies whereas untreated *P. aeruginosa* showed blackish colonies on CRA plate; it suggested that there is significant decrease in EPS production by *P. aeruginosa* when treated with *M. indicus* extract. (Fig. 4(A)).

Effect of *M. indicus* extract on EPS, rhamnolipid, and alginate production

EPS plays a crucial role in the initial stage of biofilm formation because it aids in the cell attachment and gives mechanical strength to the biofilm thus helping the bacteria towards gaining resistance against drugs. A dose-dependent decrease in EPS production of *P. aeruginosa* was noticed as 41.27 ± 3.62, 45.08 ± 2.24, and 65.36 ± 3.24%, when treated with *M. indicus* extract at the concentrations 250, 500, and 750 µg/mL respectively (Fig. 4(B)). *P. aeruginosa* is well known for

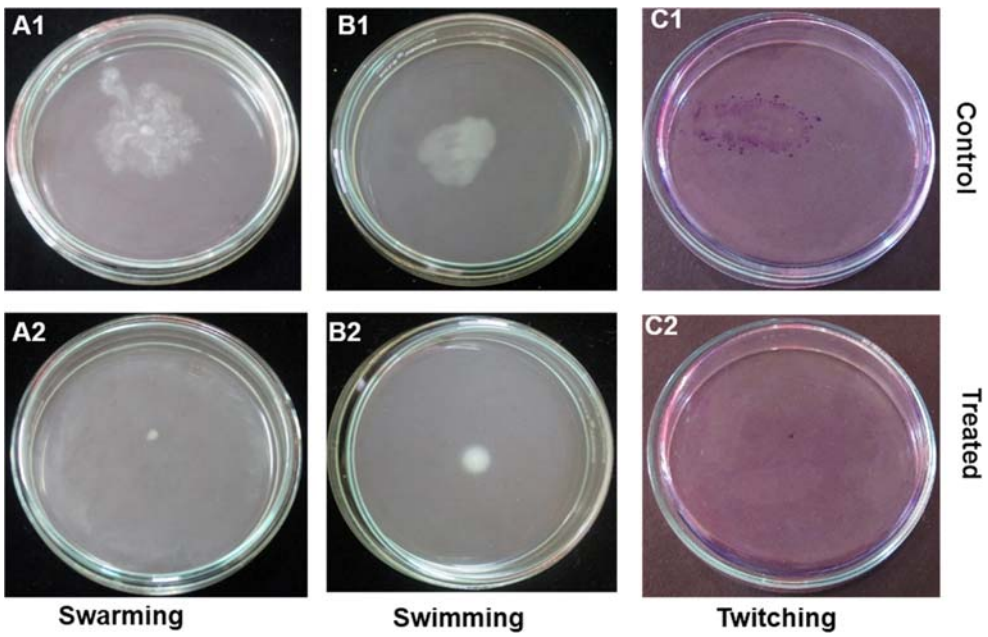

Fig. 3 Effect of *M. indicus* extract at a concentration of 750 µg/mL on motilities of *P. aeruginosa*. Swarming motility, control vs. treated with *M. indicus* extract (A1, A2); swimming motility, control vs. treated with *M. indicus* extract (B1, B2); twitching motility, control vs. treated with *M. indicus* extract (C1, C2)

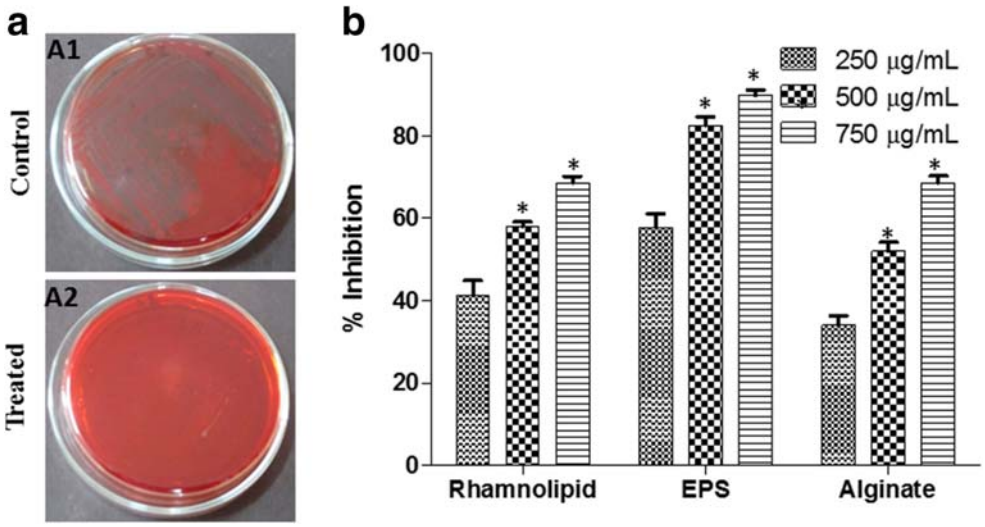

Fig. 4 (A) Effect of *M. indicus* extract at a concentration of 750 µg/mL on biofilm formation in *P. aeruginosa* by Congo red agar (CRA) method, control (A1) vs. treated with *M. indicus* extract (A2). (B) Effect of *M. indicus* extract at concentrations of 250, 500, and 750 µg/mL on rhamnolipid, EPS and alginate production in *P. aeruginosa*

production of rhamnolipid as it helps in the swarming motility by reducing the surface tension of the medium. In this experiment, rhamnolipid production was investigated. An inhibition of 41.27 ± 3.62, 57.97 ± 1.15, and 68.61 ± 1.55% in rhamnolipid production was observed on treatment with *M. indicus* extract at 250, 500, and 750 µg/mL doses respectively (Fig. 4(B)). Alginate is an exopolysaccharide synthesized by *P. aeruginosa*; it assists in unfavorable conditions and aids in adhesion to substratum. The *P. aeruginosa* treated with *M. indicus* extract showed a reduction in alginate production by 57.76 ± 3.39, 82.43 ± 2.29, and 89.79 ± 1.56% at 250, 500, and 750 µg/mL doses respectively (Fig. 4(B)).

LasA staphylolytic activity

The dose-dependent reduction was observed in staphylolytic activity of *P. aeruginosa* when treated with *M. indicus* extract because of reduction in the ability to lyse heat-killed *S. aureus* as compared with the control by 40.07 ± 0.94, 63.97 ± 1.56, and 81.19 ± 4.21% at 250, 500, and 750 µg/mL concentrations respectively (Table 1).

Quantification of reduction in biofilm formation due to *M. indicus* extract

Biofilm development by *P. aeruginosa* is hard to treat and thus leads to resistance to conventional antibiotics. On treatment of *P. aeruginosa* by *M. indicus* extract, a significant reduction in the biofilm formation was observed. At doses of 250, 500, and 750 µg/mL, the biofilms reduced by 45.03 ± 2.05, 65.93 ± 2.47, and 76.89 ± 2.24 respectively (Table 1).

CSH inhibition assay

Cell surface hydrophobicity of *P. aeruginosa* help in the colonization by adhesion to surfaces. A concomitant decrease in CSH of *P. aeruginosa* was observed when treated with increased doses of *M. indicus* extract. CSH reduced by 44.29 ± 1.78, 63.88 ± 3.63, and 68.70 ± 2.73% at the concentrations 250, 500, and 750 µg/mL respectively as compared with the untreated control (Table 1).

HCN gas production

The attribute of HCN gas production is well known in *Pseudomonas*. A significant decrease in HCN gas production was indicated by the filter paper as very less discoloration was observed when *P. aeruginosa* treated with *M. indicus* extract 750 µg/mL as compared with the negative (filter paper impregnated with solution but without *Pseudomonas aeruginosa*) and positive (without *M. indicus* extract) controls (Fig. 5(a)).

Table 1 Effect of *M. indicus* extracts (250, 500 and 750 µg/ml) on staphylolytic activity, biofilm forming activity and cell surface hydrophobicity in *P. aeruginosa*

Concentrations of *M. indicus* extracts (µg/mL)	Staphylolytic activity	Biofilm formation assay	Cell surface hydrophobicity (CSH) assay
250	40.07 ± 0.94	45.03 ± 2.05	44.29 ± 1.78
500	63.97 ± 1.56*	65.93 ± 2.47*	63.88 ± 3.63*
750	81.19 ± 4.21*	76.89 ± 2.24*	68.70 ± 2.73*

All the values were represented as Mean ± standard deviation of three replicates.

*values are significantly different from 250 µg/mL at $p<0.05$

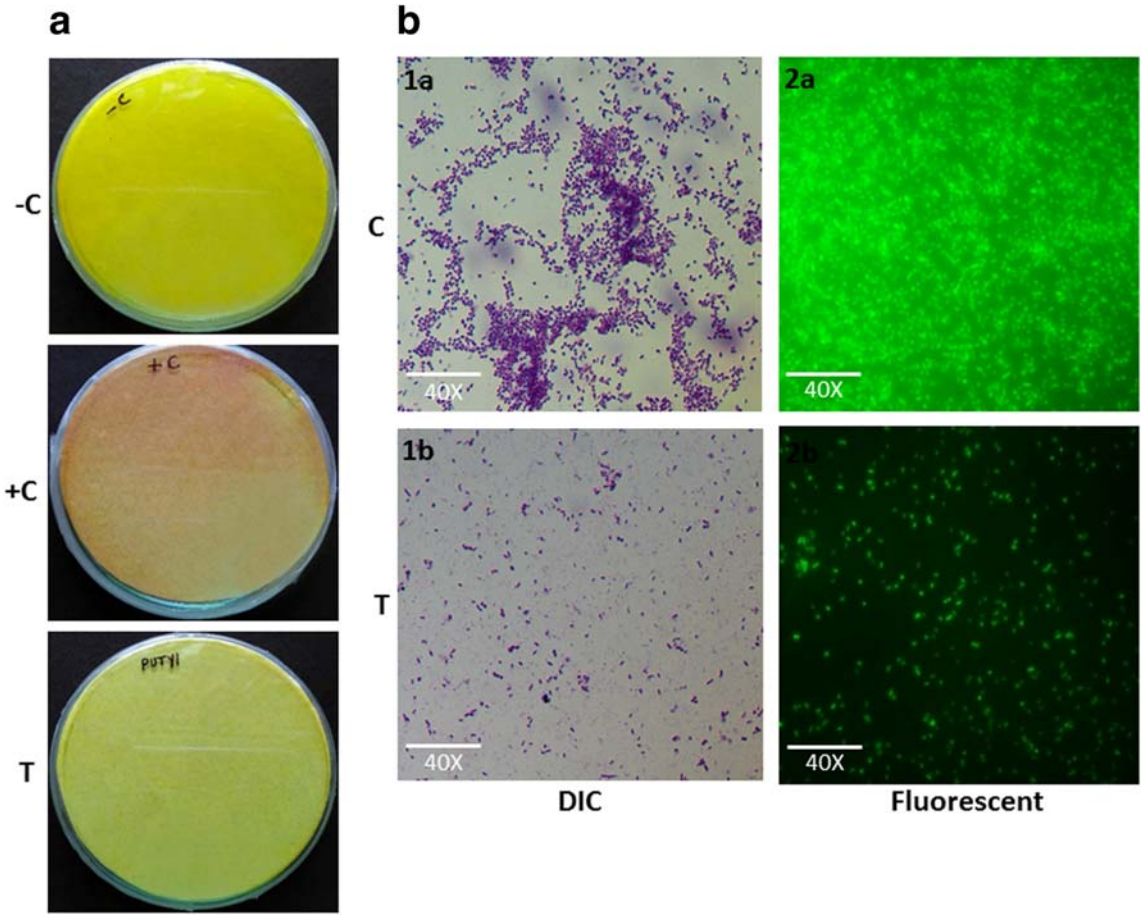

Fig. 5 (A) Effect of *M. indicus* extract at a concentration of 750 μg/mL on HCN production by *P. aeruginosa* (−C, +C, and T represent negative control, positive control, and treated with *M. indicus* extract respectively). (B) Microscopic observation of effect of *M. indicus* extract at 750-μg/mL dose on biofilm formation by *P. aeruginosa*. Differential interference contrast (DIC) microscope observation of biofilm formation by *P. aeruginosa* when treated by *M. indicus* extract (1b) in comparison with control (1a). Fluorescence microscopic observation of biofilm formation when treated by *M. indicus* extract (2b) in comparison with control (2a)

DIC and fluorescence microscopic observation of biofilm

Effect of *M. indicus* extract on the biofilm formation on glass cover slips was observed. A clear decrease in the coverage and density of bacterial cells under DIC microscope appeared which indicate the reduction in biofilm formation when it is treated with *M. indicus* extract as compared with untreated control. Likewise, a fluorescence microscopic observation of *P. aeruginosa* treated with *M. indicus* extract exhibits a significant reduction in adherence of bacterial biofilm on the glass cover slip as compared with the untreated cover slips (Fig. 5(b)).

GC-MS analysis

The compounds which are present in *M. indicus* PUTY1 extract were detected in GC-MS analysis, and their details are mentioned in Table 2. The compounds were further studied by in silico analysis.

In silico studies

Quorum sensing–regulated virulence factors and biofilm formation are controlled by its natural autoinducers 3-oxo-C12-HSL and C4-HSL interaction with LasR and RhlR respectively. In order to find out the reason behind the attenuation of quorum sensing by the *M. indicus* extract, in silico studies were carried out. Biologically active compounds detected in GC-MS study played an important role in determining the interaction of these compounds or ligands with the LasR and RhlR protein. The 2-D structures of these ligands are shown in Fig. 6. Docking score, glide energy, number of H-bond, and residues forming hydrophobic interaction were showed in great detail in Table 3. The results obtained from the docking studies revealed that phenol,2,4-bis(1,1-dimethylethyl) exhibited the maximum interaction with LasR, as observed by its docking score of − 7.95 kcal/mol, with one H-bond while the passive residues formed 12 hydrophobic and Van der Waal interactions within the catalytic site which was close to positive control, baicalein (a prominent quorum quenching agent)

Table 2 List of secondary metabolites present in the crude extract of *M. indicus* PUTY1 identified by GC-MS analysis

Sl no.	Bioactive compound	Retention time	Molecular formula	Molecular weight	Peak area (%)
1	Acetic acid, 1-methylethyl ester	2.658	$C_5H_{10}O_2$	102	1.952
2	Pyrimidine-2,4(1h,3h)-dione, 5-amino-6-nitroso	2.718	$C_4H_4O_3N_4$	156	2.223
3	Phenol, 2,4-bis(1,1-dimethylethyl)-	13.223	$C_{14}H_{22}O$	206	4.564
4	1,2-Benzenedicarboxylic acid, bis(2-methylpropyl) ester	17.129	$C_{16}H_{22}O_4$	278	8.379
5	11-Tricosene	18.295	$C_{23}H_{46}$	322	1.855
6	10-Methylanthracene-9-carboxaldehyde	18.84	$C_{16}H_{12}O$	220	49.675
7	bis(2-Ethylhexyl) maleate	19.675	$C_{20}H_{36}O_4$	340	4.025
9	1-Hexyl-1-nitrocyclohexane	21.796	$C_{12}H_{23}O_2N$	213	10.073
10	5,7-Dodecadiyn-1,12-diol	23.812	$C_{12}H_{18}O_2$	194	2.182

(Fig. 7). The docking score of 1,2-benzenedicarboxylic acid, bis(2-methylpropyl) ester, showed almost similar interactions with Tyr-56 and Tyr-64 residues of LasR with a docking score of − 5.94 kcal/mol and formed two H-bonds. Natural ligand, 3-oxo-C12-HSL, formed three H-bonds with Tyr-56, Trp-60, and Asp-73 amino acid residues of LasR. Furthermore, bis(2-ethylhexyl) maleate showed less interaction towards LasR with − 2.15 dock score and formed one H-bond with Arg48 residues. The successful molecular docking of phenol, 2,4-bis(1,1-dimethylethyl)- and 1,2-benzenedicarboxylic acid, bis(2-methylpropyl) ester with LasR transcriptional receptor, proposed that the crude extract of *M. indicus* inactivated the LasR receptor and it could be the prime mode of action against virulence factors [1].

In the case of RhlR, 1,2-benzenedicarboxylic acid, bis(2-methylpropyl) ester observed the highest docking score of − 3.24 kcal/mol and formed 1 H-bond with Trp-68, as compared with positive control Furanone C30, which has shown a docking score of − 5.13 kcal/mol (Fig. 8). Additionally, bis(2-ethylhexyl) maleate, pyrimidine-2,4(1h,3h)-dione, and 5-amino-6-nitroso also showed interaction with Arg48 and Trp68, Asp81, and Ser129 respectively with − 2.15 and − 2.05 docking scores.

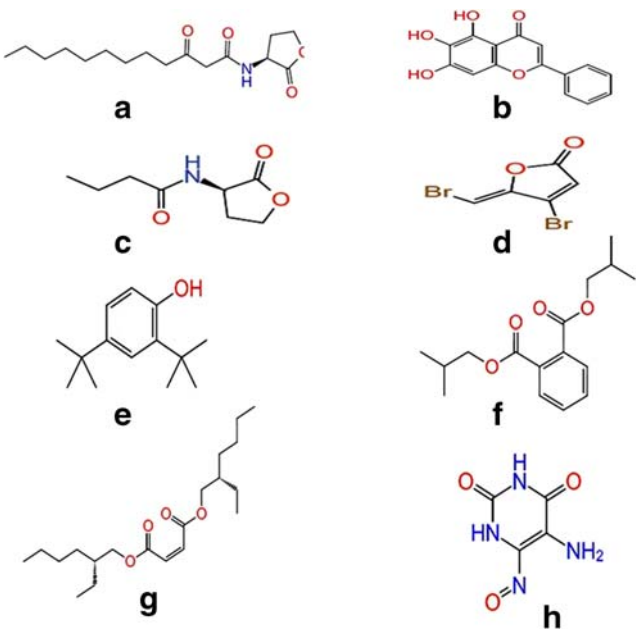

Fig. 6 Schematic representation of 2D images of (A) natural ligand for LasR (3-Oxo-C12-HSL), (B) positive control for LasR (baicalein), (C) natural ligand for RhlR (C4-HSL), (D) positive control for RhlR (furanone C30), and ligands (which were showed higher docking score), (E) phenol, 2,4-bis(1,1-dimethylethyl)-, (F) 1,2-benzenedicarboxylic acid, bis(2-Methylpropyl) ester, (G) bis 2-ethylhexyl maleate and, and H. pyrimidine-2,4(1h,3h)-dione, 5-amino-6-nitroso

Analysis of molecular dynamics simulation

Molecular docking Simulations were performed on the LasR ligand complex (positive control and ligands of fungal crude extract) and RhlR ligand complex (positive control and fungal crude extract) for 30 ns to check the stability of the complex. If the binding site residues are able to maintain the interaction with the receptor protein throughout 30-ns simulation, it depicts the stability of docked complex when compared with the positive controls. Xmgrace tool helped in plotting various graphs used in the study. RMSD of the backbone shows that the docked complex attains stability after 15 ns (Figs. 9 and 10).

Docked complexes were simulated for 30 ns with GROMACS 5.1.2 and RMSD of backbone of protein used in the study of stability of complexes of positive control LasR + P, LasR + M1, and LasR + M2 complex. It has been shown by the RMSD that the maximum deviation of the protein was 2.41 Å as compared with initial protein complex backbone (Fig. 9(A)), which means all the ensembles of the protein-ligand conformations were observed within a range of deviation 2.41 Å (higher) to 2.01 Å (stable). This showed the stability after 15 ns throughout the simulation of all complexes. RMSD of the complexes of the positive control (P) named baicalein with LasR abbreviated as LasR + P, phenol, 2,4-bis(1,1-dimethylethyl), named "M1" with LasR abbreviated as LasR + M1 and 1,2-benzenedicarboxylic acid, and bis(2-methylpropyl) ester named "M2" with LasR abbreviated

Table 3 Docking characteristics of the known natural control and positive control and identified new lead hits with receptor LasR and RhlR

		LasR						RhlR					
Sr no.	Compound name	No. of H-bond	Residues forming H-bonds	Residues forming hydrophobic and vdw interaction	Docking score (xp)	Glide energy	Glide emodel	No. of H-bond	Residues forming H-bonds	Residues forming hydrophobic and vdw interaction	Docking score (xp)	Glide energy	Glide emodel
1	Natural ligand for LasR (3-Oxo-C12-HSL)	3	Tyr56, Trp60, Asp73	L36, 40, Y47, A50, W60, Y64, V76, Y93, F101, A105, L110, G126, A127, S129	− 7.22	− 46.84	− 63.58	-	-	-	-	-	-
2	Positive control for LasR (baicalein)	3	Tyr56, Arg61, Thr75	L36, G38, A50, Y56, Y64, D73, V76, G126, A127, S129	− 8.37	− 42.61	− 60.89	-	-	-	-	-	-
3	Natural ligand for RhlR (C4-HSL)	-	-	-	-	-	-	1	Trp68	V60, Y64, L69, Y72, D81, I84, W86, L116, S129	− 3.63	− 28.23	− 37.06
4	Positive control for RhlR (furanone C30)	-	-	-	-	-	-	1	Trp68	A44, Y45, V60, H61, Y64, L69, Y72	− 5.13	− 15.96	− 15.5
5	Phenol, 2,4-bis(1,1--dimethylethyl)-	1	Thr75	L36, G38, Y47, I52, Y56, R61, Y64, D65, D73, V76, A127, S129	− 7.95	− 45.05	− 16.08	-	-	-	-	-	-
6	1,2-Benzenedicarbo-xylic acid, Bis(2-methylpropyl) ester	2	Pi-Pi, Tyr56, Tyr64	L36, G38, L39, Y47, Y56, R61, Y64, D73, T75, V76, W88, Y93, F101, A105, G126, A127, S129	− 5.94	− 28.95	− 34.43	1	Trp68	A44, Y45, G46, V60, H61, G62, Y64, L69, Y72, D81, I84, W96, L116, S135	− 3.24	− 21.75	− 35.38
7	bis(2-Ethylhexyl) maleate	-	-	L36, G38, Y47, W60, Y64, A70, D73, T75, V76, C79, W88, Y9, F101, L110, G126, A127, S129	− 4.03	− 20.7	− 23.99	1	Arg48	T58, Y72, Q73, N76, G78, A79, L85, 88, R89	− 2.15	− 31.13	− 34
8	Pyrimidine-2,4(1h,3-h)-dione, 5-amino-6-nitroso	-	-	-	-	-	-	1	Asp81	A44, Y45, V60, Y64, L69, Y72, I84	− 2.05	− 26.38	− 32.53

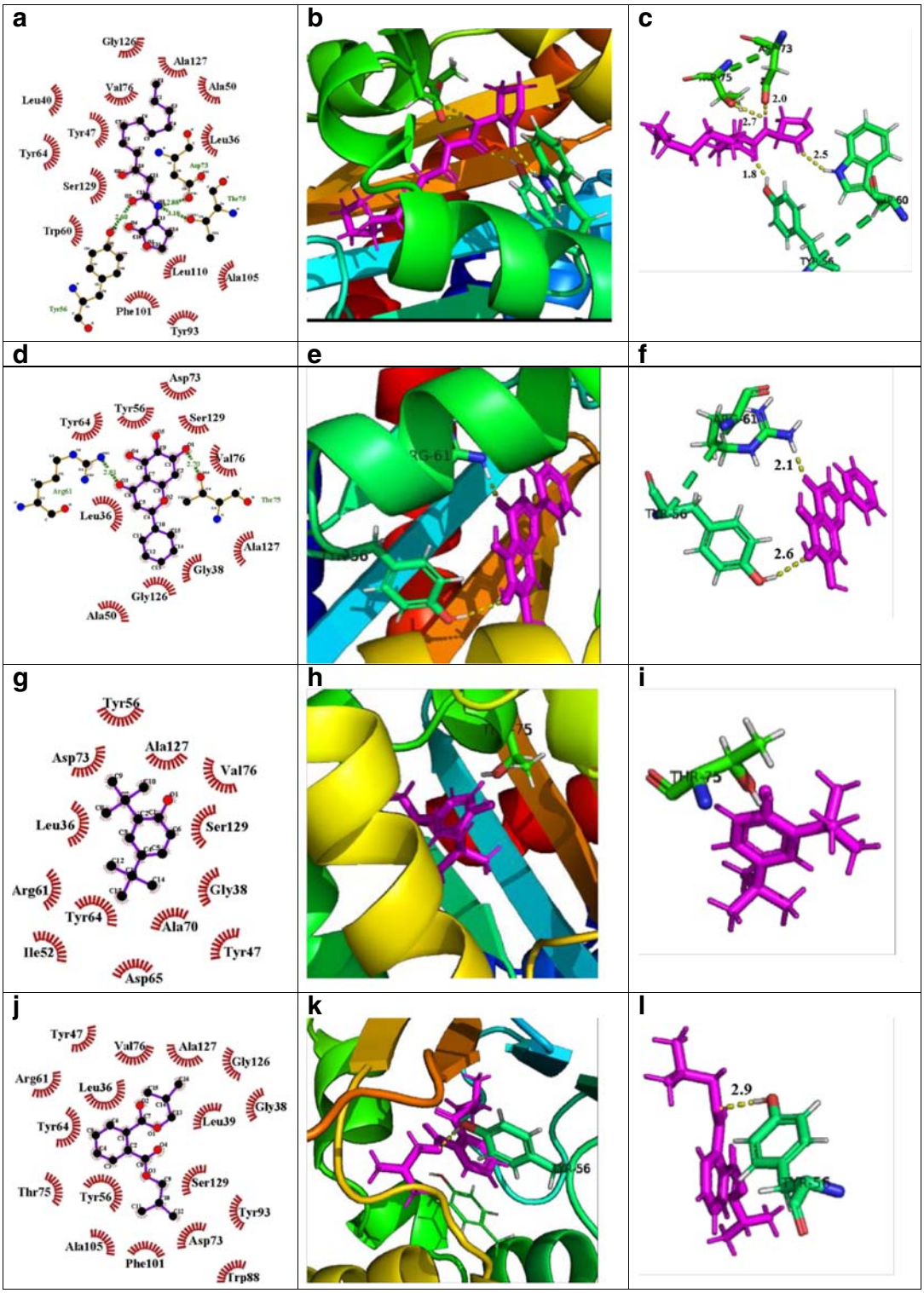

Fig. 7 Molecular docking studies of phenol, 2,4-bis(1,1-dimethylethyl)- and 1,2-benzenedicarboxylic acid, bis(2-methylpropyl) ester, bioactive components of *M. indicus* extract to investigate the interaction with the residues of active site of LasR protein, compared with natural ligand and positive control. Here, each ligand protein complex showing three images first one by LigPlot, second one by pymole, and third one by pymole (Zoomed view). (A) LigPlot view of natural ligand (C12-HSL) interacting with active site residues of LasR protein, (B) 3D view of natural ligand-LasR protein complex, (C) zoomed view, (D) LigPlot view of positive control (baicalein) interacting with active site residues of LasR, (E) 3D view of positive control LasR protein complex, (F) zoomed view, (G) LigPlot view of phenol, 2,4-bis(1,1-dimethylethyl)- interacting with active site residues of LasR, (H) 3D view of phenol, 2,4-bis(1,1-dimethylethyl)-LasR protein complex, (I) zoomed view, (J) LigPlot view of 1,2-benzenedicarboxylic acid, bis(2-methylpropyl) ester interacting with active site residues of LasR, (K) 3D view of 1,2-benzenedicarboxylic acid bis(2-methylpropyl) ester-LasR protein complex, (L) zoomed view

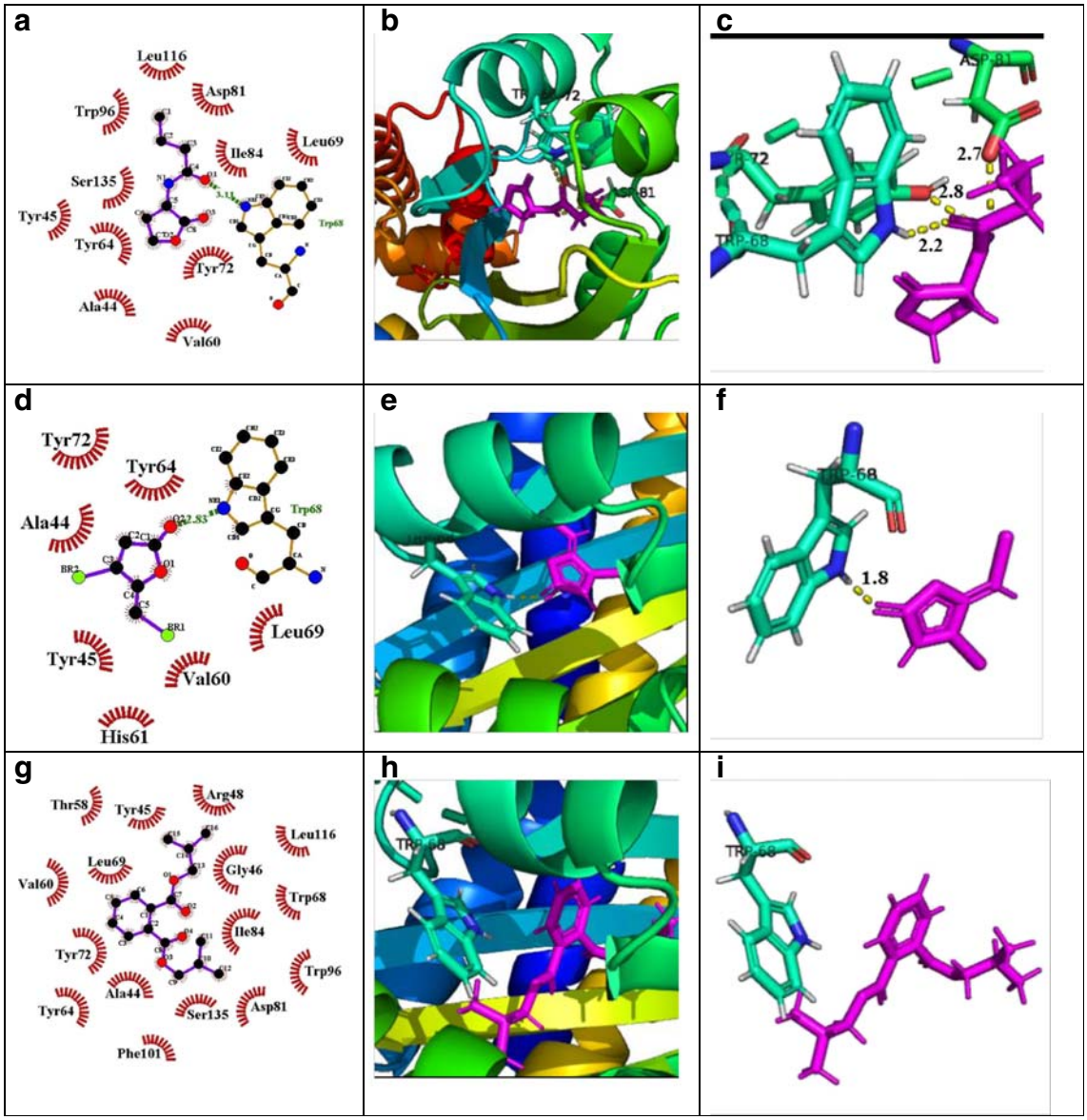

Fig. 8 Molecular docking studies of 1,2-benzenedicarboxylic Acid, bis(2-methylpropyl) ester bioactive component of *M. indicus* extract to investigate the interaction with the residues of active site of RhlR protein, as compared with natural ligand and positive control. (A) LigPlot view of natural ligand (C4-HSL) interacting with active site residues of RhlR, (B) 3D view of natural ligand-RhlR protein complex, (C) zoomed view, (D) LigPlot view of positive control (furanone C30) interacting with active site residues of RhlR, (E) 3D view of positive control-RhlR protein complex, (F) zoomed view, (G) LigPlot view of 1,2-benzenedicarboxylic acid, bis(2-methylpropyl) ester interacting with active site residues of RhlR, (H) 3D view of 1,2-benzenedicarboxylic acid, bis(2-methylpropyl) ester-RhlR protein complex, (I) zoomed view

as LasR + M2 were found to be 2.40 Å, 2.12 Å, and 2.477 Å respectively (Fig. 9(A)). LasR + M1 complex showed least deviation than the LasR + M2 and positive control whereas LasR + M1 showed similar RMSD to positive control after 15 ns. Therefore, M1 could be considered as the best inhibitor than the M2 and positive control while M2 similar to positive control. Residue fluctuations of the amino acids were calculated, with respect to the initial stage by applying the root mean square fluctuations (RMSF) (Fig. 9(B)). The local changes in the structure during the MD simulations can be achieved with the help of RMSF. A sharp peak in the RMSF plot indicated that the residues exhibit more fluctuations during simulations. The dimensions of an object can be described with the help of "Radius of gyration" by calculating the RMSD between center of gravity and its ends. Radius of gyration provides an indication to the level of compaction in the structures and also aids in the measurement of the stability of the folded protein. Radius of the initial starting structure was 1.52 nm which decreased up to 1.44 nm at the end of 30 ns and MD simulations showed that protein-ligand complex was stable and well folded (Fig. 9(C)). During the MD simulations, it has been observed that an average protein complex has 1–4 H-bonds between the ligand and receptor complex (Fig. 9(D)).

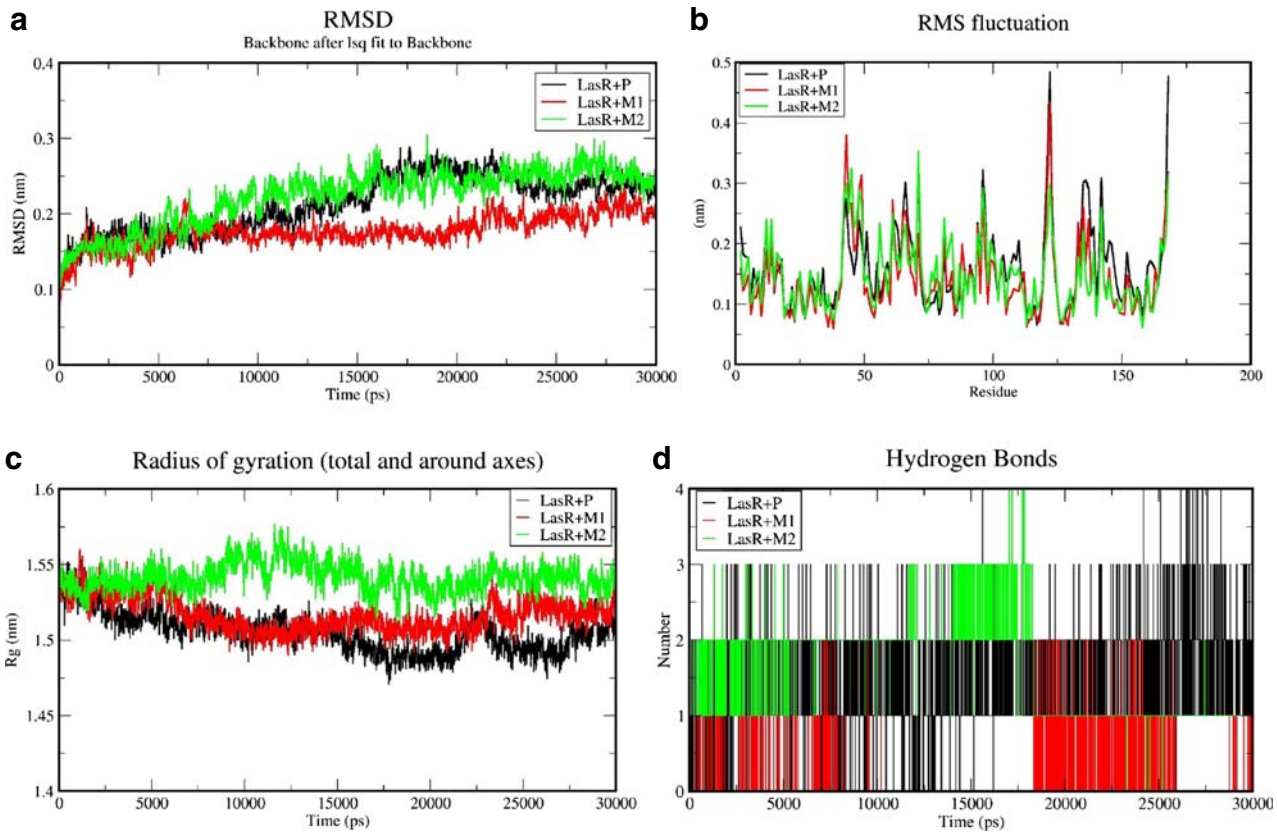

P (Positive Control i.e. Baicalein); M1 (Phenol, 2,4-Bis(1,1-Dimethylethyl)-); M2 (1,2-Benzenedicarboxylic Acid, Bis(2-Methylpropyl) Ester).

Fig. 9 Analysis backbone trajectory of the LasR-complexes onwards. (A) RMSD, (B) RMSF, (C) radius of gyration, and (D) H-bond

In the case of RhlR ligand complex, RMSD showed the maximum deviation (Fig. 10(P)) of the protein as 4.389 Å (0.4389 nm) compared with the initial protein complex backbone. This means all the ensembles of the protein-ligand conformations were observed within a range of deviation 6.281 (higher) to 4.675 Å (stable). RMSD values of the positive control, and (ligands of fungal crude extract) 1,2-benzenedicarboxylic acid, bis(2-methylpropyl) ester abbreviated as RhlR + N1 and bis(2-ethylhexyl) maleate abbreviated as RhlR + N2 were found to be 6.281 Å, 7.620 Å, and 5.695 Å respectively (Fig. 10(P)). RhlR + N1 and RhlR + N2 complex showed approximately similar deviation from 10 to 30 ns but both the complexes showed less deviation than the RhlR + P (positive control). Simultaneously positive control showed least stable RMSD compared with N1 and N2 complexed of RhlR. Therefore, N1 could be considered as the best inhibitor than the positive control and because N2 has been reported as a toxic molecule. RMSF plot indicated that the residues also show less fluctuation compared with positive control during simulations (Fig. 10(Q)), which shows that interacting residue interacting with the ligand during simulation. Radius of the initial starting structure was 2.1696 nm which decreased up to 2.0441 nm at the end of 30 ns and MD simulations showed that protein-ligand complex was stable and well folded (Fig. 10(R)). It has been observed that N1 and N2 showed more no of an average 1–5 H-bonds between ligand protein complex as compared with complex of positive control (RhlR + P) which showed its better binding to receptor with ligand N1and N2 than the positive control (Fig. 10(S)).

Discussion

Biofilm is a well-organized community of microbial cells, can be formed on animate or inanimate objects, and is surrounded by self-secreted biopolymers. Biofilm-associated microbial infections are usually hard to eradicate due to the emergence of multi-drug-resistant strains. *P. aeruginosa* is well known for biofilm formation and it can form a potent biofilm even anaerobic condition as in cystic fibrosis patients. Hence, there is an ever-growing need to identify and explore the hidden bioactive molecules which act against microbial biofilm formation. Quorum quenching is one of the effective strategies for targeting the microbial quorum sensing pathways to

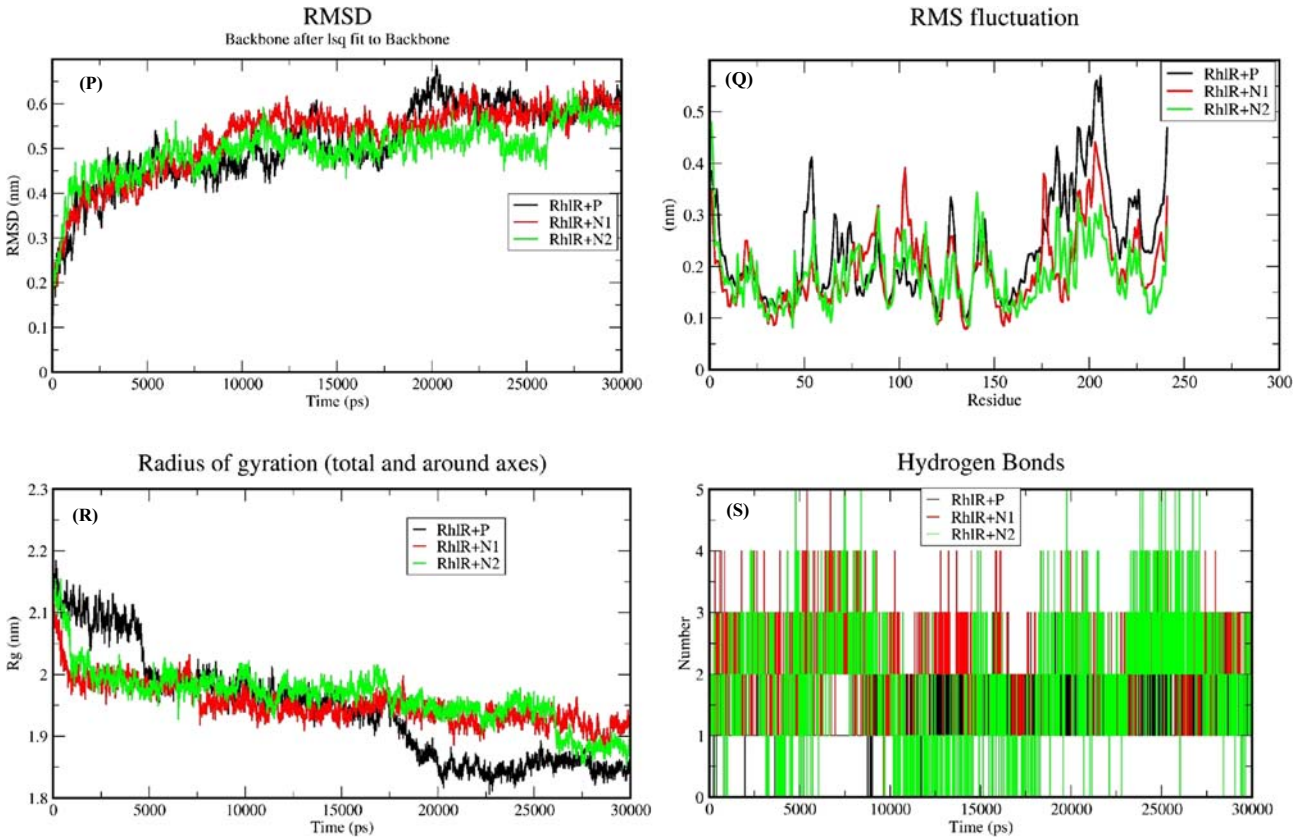

P (Positive Control i.e. Furanone C30); N1 (1,2-Benzenedicarboxylic Acid, Bis(2-Methylpropyl) Ester); N2 (Bis(2-Ethylhexyl) Maleate).

Fig. 10 Analysis backbone trajectory of the RhlR complexes onwards. (P) RMSD (Q) RMSF (R) Radius of gyration, and (S) H-bond

prevent the virulence and biofilm formation of *P. aeruginosa*. In this report, the quorum quenching competence of biologically active secondary metabolites of *M. indicus* extract against *P. aeruginosa* was investigated. On the basis of morphological and molecular phylogenetic analyses, the shortlisted fungal culture PUTY1 was identified as *Mycoleptodiscus indicus* PUTY1 (KY550710.1) which formed a distinct monophyletic clade with other *M. indicus* strains. *Mycoleptodiscus indicus*, a dematiaceous hyphomycete, has occasionally been reported as pathogenic because it rarely infects human beings. Until now, only 3 cases have been reported and all probably initiated by direct transmission of *M. indicus* from the floral part [47]. *M. indicus* PUTY1 has been isolated for the first time from *Tridax procumbens*. In addition, secondary metabolites produced by *M. indicus* showed significant antivirulence activities against *Pseudomonas aeruginosa*. Andrioli et al. (2014) reported three azaphilones from *M. indicus* viz. mycoleptones A, B, and C, isolated from the host *Borreria verticillata*. Besides, four polyketides, such as austdiol, eugenitin, 6-methoxyeugenin, and 9-hydroxyeugenin, were also reported from the same fungi [48]. Various biological activities have been found in azaphilones like antibacterial, antifungal, antioxidant, antiviral, nematocidal, and anti-inflammatory [49, 50].

In this study, a preliminary screening was performed against the model organism, i.e., *Chromobacterium violaceum* to check the quantitative violacein inhibition to evaluate the quorum quenching potential of *M. indicus* extract. When the concentration of *M. indicus* extract increased, the production of violacein decreased significantly. Current finding is in agreement to the previous study where dose-dependent inhibition in violacein production was recorded [51].Growth curve analysis showed that *P. aeruginosa* treated with *M. indicus* extract, produced a similar sigmoid curve as in the untreated control which suggests that it is not affecting the viability of the cells at sub-MIC dose [27]. Virulence factor like pyocyanin which is regulated by rhl system of *P. aeruginosa* responsible for acute oxidative damage to the internal organs such as lungs and impaired ciliary functions in the patients. *M. indicus* extract exhibited significant dose-dependent reduction in pyocyanin production by 75.21 ± 2.31% at 750 μg/mL. The same activity of pyocyanin inhibition has been found in *Terminalia chebula* extract [52].

Ex vivo result showed that elastase producing isolates of *P. aeruginosa* significantly aid in damaging the skin and wound by degrading the skin proteins [53] and thus aid in the pathogenicity. Hence, elastase assay was also performed. This study showed a significant decrease in elastase production when treated with *M. indicus* extract. A similar elastase reduction was reported by Zhou et al. [54] where *Plectosphaerella cucumerina*, isolated from *Orychophragmus violaceus*, showed 42% reduction in elastase production against *P. aeruginosa* at a dose of 1 mg/mL [28]. *P. aeruginosa* also produces a hydrolytic enzyme, protease, which helps in the colonization of host tissues in unfavorable conditions [27]. The protease is another deadly virulence factor secreted by this bacterium that degrades the proteins of infected tissues in the host and facilitates growth and invasion of bacteria [55]. In the present study, *M. indicus* extract showed significant attenuation in protease production as shown in the figure (Fig. 2(B)). This result of ours corroborates with that of a previous finding depicting the fungal secondary metabolites from *Plectosphaerella cucumerina* attenuating protease activity significantly [54].

It has been reported that higher swarming motility facilitates microbial biofilm formation efficiently [56]. Due to the strong correlation between motility and bacterial colonization on the surface, we checked the effect of *M. indicus* extract on bacterial movement. Results indicated adequacy of PUTY1 crude extract in diminishing the swimming, swarming, and twitching motility as compared with the control of swimming, swarming, and twitching (Fig. 3).

Formation of biofilm and development of MDR strains are primarily responsible for ineffectiveness of antibiotic therapy in patients infected by *Pseudomonas aeruginosa* [57]. In this context, efficacy of *M. indicus* extract on biofilm formation by this bacterium was tested on Congo red agar. The control, which was devoid of *M. indicus* extract, showed black crystalline colonies due to the EPS formation that aids in the development of biofilm. However, in the presence of increasing concentrations of *M. indicus* (PUTY1) extract, the organism was unable to form biofilm and black-colored colonies were not observed, indicating the absence of formation of EPS [31].

In biofilm formation, rhamnolipids have an important role, as they modulate the swarming and colonization of incipient biofilm formation. Moreover, *M. indicus* extract significantly downregulates the production of rhamnolipid in *P. aeruginosa* in a dose-dependent manner. The downregulation of rhamnolipid showed the potential of *M. indicus* extracts against quorum sensing as rhamnolipid promotes maturation of biofilm and play important role in chronic infections by immune evasion [58]. Alginate is a key constituent of EPS and aids in maintaining the integrity and architecture of biofilm and provides resistance against drugs by hindering its access. Furthermore, it has been supported by animal studies that it takes part in tissue damage, promotes existence in the lungs, and hinders host immune clearance [59]. Therefore, we also checked the effect of *M. indicus* extract on alginate production. A significant decrease in alginate was observed, which is in accordance with earlier findings [60].

M. indicus extract also acted on the early stage of the biofilm development by decreasing CSH and EPS. Generally, HCN gas production begins at a late exponential phase or at the start of stationary phase because it is QS-dependent [61]. A significant reduction in HCN production was observed after treatment with *M. indicus* extract as compared with the negative (impregnated with solution but without *Pseudomonas aeruginosa*) and positive (without *M. indicus* extract) controls (Fig. 5(a)). The ability of *M. indicus* extract to reduce the biofilm formation was also confirmed by microscopic observations, illustrating significant reduction in adherence of bacterial cells on the glass cover slip when compared with the dense biofilm in the control (Fig. 5(b)).

The GC-MS analysis revealed the biologically active compounds, which were present in *M. indicus* extract in different proportions. The main potential components present in *M. indicus* extract were 10-methylanthracene-9-carboxaldehyde, 1-hexyl-1-nitrocyclohexane, 1,2-benzenedicarboxylic acid, bis(2-methylpropyl) ester, phenol, 2,4-bis(1,1-dimethylethyl)-, and bis(2-ethylhexyl) maleate. The details of compounds present in *M. indicus* extract are shown in Table 2. The compound 1-hexyl-1-nitrocyclohexane found in GC-MS analysis in the crude extract was reported to have biological activities such as antioxidant, antimicrobial, and anti-inflammatory from the methanolic leaf extract of *Eupatorium triplinerve*, a medicinal plant [62]. The compound phenol, 2,4-bis(1,1-dimethylethyl) also called 2,4-di-tert butylphenol (DTBP), present in the *M. indicus* extract has shown a peak area percentage of 4.564 in the GC-MS analysis. This indicates its efficiency in conferring biological activities and active quenching of the QS-controlled virulence factors and biofilm formation. DTBP is known to have diverse therapeutic activities as reported in previous studies, including antimalarial [63]. antibacterial, antifungal, anticancer, and antioxidant activities [64]. This is the first report of this compound to be reported in *M. indicus* extracts. Further, the presence of 1,2-benzenedicarboxylic acid, bis(2-methylpropyl) ester in the *M. indicus* extract also gave an insight into its possible role in quorum quenching due to its therapeutic nature of antimicrobial activity [65]. The present study has demonstrated that *M. indicus* extracts exhibited significant quorum quenching activities against virulence factors and biofilm formation, which are regulated by LasI/R and RhlI/R QS systems of *P. aeruginosa*.

The in vitro experiments of quorum quenching indicate that the *M. indicus* extracts have a great potential in downregulating the virulence of *P. aeruginosa* by significantly altering the expression of its corresponding genes. As shown in the

results, a concentration-dependent reduction was found in staphylolytic activity of *P. aeruginosa* when treated with *M. indicus* extracts. This finding is in agreement with the previous studies [36]. Besides these, *M. indicus* extracts also exhibited significant potential against biofilm formation as evidenced from both crystal violet micro titer plates and microscopic observations, which depict its importance in the alteration of bacterial tolerance to conventional antibiotics. An array of bioactive constituents was reported by means of GC-MS analysis.

The importance of bioactive constituents produced by *M. inducus*, found in GC-MS analysis, in the attenuation of quorum sensing associated virulence was further validated by "in silico studies." Mode of action of bioactive constituents has been well depicted by the molecular docking studies due to inactivation of the LasR and RhlR transcriptional receptor proteins. In silico analysis showed the mechanism of compounds present in the *M. indicus* extract in quorum quenching. Docking analysis with LasR protein exhibited that phenol, 2,4-bis(1,1-dimethylethyl), a known quorum sensing agent, binds firmly to the LasR protein, which was close to docked score of the natural ligand 3-Oxo-C12-HSL. Also, 1,2-benzenedicarboxylic acid, bis(2-methylpropyl) ester has shown a very good docking score and formed 2H-bond with Tyr-56, and Tyr-64. Molecular dynamics–based trajectory analysis has shown an energetically stable conformation of LasR proteins with their corresponding ligand complexes. RMSD profile showed that all the complexes attained their equilibrium after 15 ns (Fig. 9). It has been noticed that phenol, 2,4-bis(1,1-dimethylethyl)-LasR complex revealed a proper steady pattern after 15 ns followed by 1,2-benzenedicarboxylic acid, bis(2-methylpropyl) ester with some fluctuations. Both were showed better stability pattern than the positive control.

In terms of RhlR, 1,2-benzenedicarboxylic acid, bis(2-methylpropyl) ester, showed the highest, i.e., − 3.24, docking score which was similar to natural ligand of RhlR. After that, bis(2-ethylhexyl) maleate showed − 2.15 docking score, which was less than the natural ligand of RhlR.

In RMSD, the 1,2-benzenedicarboxylic acid, bis(2-methylpropyl) ester-RhlR complex, exhibited initial fluctuations up to ~ 10 ns and then showed stable conformation after ~ 12 ns. However, in RhlR-bis(2-ethylhexyl) maleate complex, a steady pattern was observed after ~ 15 ns (Fig. 10). The present study provides alternative strategies to develop the potent quorum sensing inhibitors from unexplored fungal secondary metabolites.

Conclusions

The present study reveals that *M. indicus* extracts exhibit significant decrease in QS-regulated virulence factors and biofilm formation in *P. aeruginosa*. This suggests that *M. indicus* extracts play a critical role in downregulating the QS-regulated genes resulting in significant alterations in the production of virulence factors. Additionally, *M. indicus* extracts also exhibited a significant reduction in the biofilm formation as evidenced from the microscopic observations. The potential of bioactive component of *M. indicus* extracts, obtained from GC-MS analysis, was further confirmed by in silico analysis. The in silico studies have shown that the compounds present in the *Mycoleptodiscus indicus* extract such as phenol, 2,4-bis(1,1-dimethylethyl)-, showed binding affinity with LasR protein whereas 1,2 benzenedicarboxylic acid, bis(2-methylpropyl) ester showed binding affinity with both the proteins, LasR and RhlR, to mitigate the QS of *P. aeruginosa*. Thus, the present study unfolds alternative strategies for the exploitation of effective quorum sensing inhibitors (QSIs) from unexplored natural resources. Additionally, the current study also unfolds new possibilities in the application and evolution of secondary metabolites of fungal origin as antimicrobial agents in the post-antibiotic period. Future research endeavors should focus on purification of the potent compounds, which may enhance our understanding towards fungal secondary metabolites as one of the natural sources.

Acknowledgments The first author would like to thank the Pondicherry University for a fellowship. The Department of Biotechnology, Pondicherry University, is thanked for providing the facilities. The partial infrastructural support from UGC-SAP and DST-FIST programs are thanked.

Funding The Pondicherry University provided a fellowship to the first author.

Compliance with ethical standards

Conflict of interest The authors declare that they have no conflict of interest.

References

1. Maisuria VB, Lopez-de Los Santos Y, Tufenkji N, Déziel E (2016) Cranberry-derived proanthocyanidins impair virulence and inhibit quorum sensing of *Pseudomonas aeruginosa*. Sci Rep 6: 30169, https://doi.org/10.1038/srep30169 (2016)
2. Geddes A (2000) Infection in the twenty-first century: predictions and postulates. J Antimicrob Chemother 46:873–877. https://doi.org/10.1093/jac/46.6.873
3. Borges A, Sousa P, Gaspar A, Vilar S, Borges F, Simões M (2017) Furvina inhibits the 3-oxo-C12-HSL-based quorum sensing system of *Pseudomonas aeruginosa* and QS-dependent phenotypes. Biofouling 33:156–168. https://doi.org/10.1080/08927014.2017.1280732
4. Chastre J, Fagon JY (2002) Ventilator-associated pneumonia. Amer J Res and Crit care med 165:867–903. https://doi.org/10.1164/ajrccm.165.7.2105078

5. Hutchison ML, Govan JR (1999) Pathogenicity of microbes associated with cystic fibrosis. Microb Infect 1:1005–1014. https://doi.org/10.1016/S1286-4579(99)80518-8
6. Lyczak JB, Cannon CL, Pier GB (2000) Establishment of *Pseudomonas aeruginosa* infection: lessons from a versatile opportunist. Microb and Infect 2:1051–1060. https://doi.org/10.1016/S1286-4579(00)01259-4
7. Costerton JW, Stewart PS, Greenberg EP (1999) Bacterial biofilms: a common cause of persistent infections. Science 284:1318–1322. https://doi.org/10.1126/science.284.5418.1318
8. Middleton B, Rodgers HC, Cámara M, Knox AJ, Williams P, Hardman A (2002) Direct detection of N-acylhomoserine lactones in cystic fibrosis sputum. FEMS Microbiol Lett 207:1–7. https://doi.org/10.1111/j.1574-6968.2002.tb11019.x
9. Bhagirath AY, Li Y, Patidar R, Yerex K, Ma X, Kumar A, Duan K (2019) Two component regulatory systems and antibiotic resistance in gram-negative pathogens. Int j of mol sci 20:1781
10. Lingzhi L, Haojie G, Dan G, Hongmei M, Yang L, Mengdie J, Xiaohui Z (2018) The role of two-component regulatory system in β-lactam antibiotics resistance. Microbiol Res 215:126–129
11. Parkins MD, Ceri H, Storey DG (2001) *Pseudomonas aeruginosa* GacA, a factor in multihost virulence, is also essential for biofilm formation. Mole microbiol 40:1215–1226
12. Lee J, Wu J, Deng Y, Wang J, Wang C, Wang J, Chang C, Dong Y, Williams P, Zhang LH (2013) A cell-cell communication signal integrates quorum sensing and stress response. Nat Chem Biol 9:339–343. https://doi.org/10.1038/nchembio.1225
13. Willcox MDP, Zhu H, Conibear TCR, Hume EBH, Givskov M, Kjelleberg S, Rice SA (2008) Role of quorum sensing by *Pseudomonas aeruginosa* in microbial keratitis and cystic fibrosis. Microbiology 154:2184–2194. https://doi.org/10.1099/mic.0.2008/019281-0
14. Luo J, Biying D, Ke W, Shuangqi C, Tangjuan L, Xiaojing C, Danqing L (2017) Baicalin inhibits biofilm formation, attenuates the quorum sensing-controlled virulence and enhances Pseudomonas aeruginosa clearance in a mouse peritoneal implant infection model. PLoS One 12:e0176883. https://doi.org/10.1371/journal.pone.0176883
15. Vandeputte OM, Martin K, Tsiry R, Caroline S, Pierre D, Sanda R, Billo D, Adeline M, Marie B, Mondher E (2011) The flavanone naringenin reduces the production of quorum sensing-controlled virulence factors in Pseudomonas aeruginosa PAO1. Microbiology 157:2120–2132. https://doi.org/10.1099/mic.0.049338-0
16. Vasavi HS, Sudeep HV, Lingaraju HB, Prasad KS (2017) Bioavailability-enhanced Resveramax™ modulates quorum sensing and inhibits biofilm formation in *Pseudomonas aeruginosa* PAO1. Microb Pathog 104:64–71. https://doi.org/10.1016/j.micpath.2017.01.015
17. Bills GF, Polishook JD (1994) Abundance and diversity of microfungi in leaf litter of a lowland rain forest in Costa Rica. Mycologia 86:187–198. https://doi.org/10.2307/3760635
18. Patil MP, Patil RH, Maheshwari VL (2015) Biological activities and identification of bioactive metabolite from endophytic *Aspergillus flavus* L7 isolated from *Aegle marmelos*. Curr Microbiol 71:39–48. https://doi.org/10.1007/s00284-015-0805-y
19. Oliveira BDÁ, Rodrigues AC, Cardoso BMI, Ramos ALCC, Bertoldi MC, Taylor JG, da Cunha LR, Pinto UM (2016) Antioxidant, antimicrobial and anti-quorum sensing activities of *Rubus rosaefolius* phenolic extract. Ind Crop Prod 84:59–66. https://doi.org/10.1016/j.indcrop.2016.01.037
20. Dolatabad HK, Javan-Nikkhah M, Shier WT (2017) Evaluation of antifungal, phosphate solubilisation, and siderophore and chitinase release activities of endophytic fungi from *Pistacia vera*. Mycol Prog 16:777–790. https://doi.org/10.1007/s11557-017-1315-z
21. Huelsenbeck JP, Ronquist F (2001) MRBAYES: Bayesian inference of phylogenetic trees. Bioinformatics 17:754–755. https://doi.org/10.1093/bioinformatics/17.8.754
22. Zhaxybayeva O, Gogarten JP (2002) Bootstrap, Bayesian probability and maximum likelihood mapping: exploring new tools for comparative genome analyses. BMC Genomics 3:4. https://doi.org/10.1186/1471-2164-3-4
23. Stamatakis A, Hoover P, Rougemont J (2008) A rapid bootstrap algorithm for the RAxML web servers. Syst Boil 57:758–771. https://doi.org/10.1080/10635150802429642
24. Miller MA, Pfeiffer W, Schwartz T (2010) Creating the CIPRES science gateway for inference of large phylogenetic trees. In Gateway Computing Environments Workshop (GCE):1–8. https://doi.org/10.1109/GCE.2010.5676129
25. Husain FM, Ahmad I, Al-thubiani AS, Abulreesh HH, AlHazza IM, Aqil F (2017) Leaf extracts of *Mangifera indica* L. inhibit quorum sensing–regulated production of virulence factors and biofilm in test bacteria. Front Microbial 8:727. https://doi.org/10.3389/fmicb.2017.00727
26. Sethupathy S, Shanmuganathan B, Kasi PD, Pandian SK (2016) Alpha-bisabolol from brown macroalga *Padina gymnospora* mitigates biofilm formation and quorum sensing controlled virulence factor production in *Serratia marcescens*. J Appl Phycol 28:1987–1996. https://doi.org/10.1007/s10811-015-0717-z
27. Luo J, Kong JL, Dong BY, Huang H, Wang K, Wu LH, Hou CC, Liang Y, Li B, Chen YQ (2016) Baicalein attenuates the quorum sensing-controlled virulence factors of *Pseudomonas aeruginosa* and relieves the inflammatory response in *P. aeruginosa*-infected macrophages by downregulating the MAPK and NFκB signal-transduction pathways. Drug Des Dev Ther 10:183. https://doi.org/10.2147/DDDT.S97221
28. Das MC, Sandhu P, Gupta P, Rudrapaul P, De UC, Tribedi P, Akhter Y, Bhattacharjee S (2016) Attenuation of *Pseudomonas aeruginosa* biofilm formation by vitexin: a combinatorial study with azithromycin and gentamicin. Sci Rep 6:23347. https://doi.org/10.1038/srep23347
29. Packiavathy IASV, Priya S, Pandian SK, Ravi AV (2014) Inhibition of biofilm development of uropathogens by curcumin–an anti-quorum sensing agent from *Curcuma longa*. Food Chem 148:453–460. https://doi.org/10.1016/j.foodchem.2012.08.002
30. Roudashti S, Zeighami H, Mirshahabi H, Bahari S, Soltani A, Haghi F (2017) Synergistic activity of sub-inhibitory concentrations of curcumin with ceftazidime and ciprofloxacin against *Pseudomonas aeruginosa* quorum sensing related genes and virulence traits. World J Microbiol Biotechnol 33:50. https://doi.org/10.1007/s11274-016-2195-0
31. Chhibber S, Gondil VS, Sharma S, Kumar M, Wangoo N, Sharma RK (2017) A novel approach for combating *Klebsiella pneumoniae* biofilm using histidine functionalized silver nanoparticles. Front Microbiol 8:1104. https://doi.org/10.3389/fmicb.2017.01104
32. Rasamiravaka T, Ngezahayo J, Pottier L, Ribeiro SO, Souard F, Hari L, Stévigny C, Jaziri ME, Duez P (2017) Terpenoids from *Platostoma rotundifolium* (Briq.) AJ Paton alter the expression of quorum sensing-related virulence factors and the formation of biofilm in *Pseudomonas aeruginosa* PAO1. Int J Mol Sci 18:1270. https://doi.org/10.3390/ijms18061270
33. Gupta P, Sarkar A, Sandhu P, Daware A, Das MC, Akhter Y, Bhattacharjee S (2017) Potentiation of antibiotic against *Pseudomonas aeruginosa* biofilm: a study with plumbagin and gentamicin. J Appl microbial 123:246–261. https://doi.org/10.1111/jam.13476
34. Kalia M, Yadav VK, Singh PK, Sharma D, Pandey H, Narvi SS, Agarwal V (2015) Effect of cinnamon oil on quorum sensing-controlled virulence factors and biofilm formation in *Pseudomonas aeruginosa*. PLoS One 10:e0135495. https://doi.org/10.1371/journal.pone.0135495

35. Knutson CA, Jeanes A (1968) A new modification of the carbazole analysis: application to heteropolysaccharides. Anal Biochem 24: 470–481. https://doi.org/10.1016/0003-2697(68)90154-1
36. Alasil SM, Omar R, Ismail S, Yusof MY (2015) Inhibition of quorum sensing-controlled virulence factors and biofilm formation in *Pseudomonas aeruginosa* by culture extract from novel bacterial species of *Paenibacillus* using a rat model of chronic lung infection. Inter J Bacteriol:2015. https://doi.org/10.1155/2015/671562
37. Luciardi MC, Blázquez MA, Cartagena E, Bardón A, Arena ME (2016) Mandarin essential oils inhibit quorum sensing and virulence factors of *Pseudomonas aeruginosa*. LWT-Food Sci Technol 68:373–380. https://doi.org/10.1016/j.lwt.2015.12.056
38. García-Lara B, Saucedo-Mora MÁ, Roldán-Sánchez JA, Pérez-Eretza B, Ramasamy M, Lee J, Coria-Jimenez R, Tapia M, Varela-Guerrero V, García-Contreras R (2015) Inhibition of quorum-sensing-dependent virulence factors and biofilm formation of clinical and environmental *Pseudomonas aeruginosa* strains by ZnO nanoparticles. Lett Appl Microbiol 61:299–305. https://doi.org/10.1111/lam.12456
39. Ghodsalavi B, Ahmadzadeh M, Soleimani M, Madloo PB, Taghizad-Farid R (2013) Isolation and characterization of rhizobacteria and their effects on root extracts of *Valeriana officinalis*. Aust J Crop Sci 7:338
40. Lovell SC, Davis IW, Arendall WB III, De Bakker PI, Word JM, Prisant MG, Richardson JS, Richardson DC (2003) Structure validation by Cα geometry: ϕ, ψ and Cβ deviation. Proteins: Strut Funct Bioinf 50:437–450. https://doi.org/10.1002/prot.10286
41. Vriend G (1990) WHAT IF: a molecular modeling and drug design program. J Mol Graph 8:52–56. https://doi.org/10.1016/0263-7855(90)80070-V
42. Schüttelkopf AW, Van Aalten DM (2004) PRODRG: a tool for high-throughput crystallography of protein–ligand complexes. Acta Crystallogr D Biol Crystallogr 60:1355–1363. https://doi.org/10.1107/S0907444904011679
43. Hess B, Bekker H, Berendsen HJ, Fraaije JG (1997) LINCS: a linear constraint solver for molecular simulations. J Comput Chem 18:1463–1472. https://doi.org/10.1002/(SICI)1096-987X(199709)18:12<1463::AID-JCC4>3.0.CO;2-H
44. Miyamoto S, Kollman PA (1992) Settle: an analytical version of the SHAKE and RATTLE algorithm for rigid water models. J Comput Chem 13:952–962. https://doi.org/10.1002/jcc.540130805
45. Darden T, York D, Pedersen L (1993) Particle mesh Ewald: an N·log (N) method for Ewald sums in large systems. J Chem Phys 98: 10089–10092. https://doi.org/10.1063/1.464397
46. Parrinello M, Rahman A (1981) Polymorphic transitions in single crystals: a new molecular dynamics method. J Appl Phys 52:7182–7190. https://doi.org/10.1063/1.328693
47. Koo S, Sutton DA, Yeh WW, Thompson EH, Sigler L, Shearer JF, Hofstra DE, Wickes BL, Marty FM (2012) Invasive *Mycoleptodiscus* fungal cellulitis and myositis. Med Mycol 50: 740–745. https://doi.org/10.3109/13693786.2012.656717
48. Andrioli WJ, Conti R, Araújo MJ, Zanasi R, Cavalcanti BC, Manfrim V, Toledo JS, Tedesco D, de Moraes MO, Pessoa C, Cruz AK (2014) Mycoleptones A–C and Polyketides from the Endophyte *Mycoleptodiscus indicus*. J Nat Prod 77:70–78. https://doi.org/10.1021/np4006822
49. Colombo L, Gennari C, Ricca GS, Scolastico C, Aragozzini F (1981) Detection of one symmetrical precursor during the biosynthesis of the fungal metabolite austdiol using [1, 2-13 C 2] acetate and [me-13 C] methionine. J Chem Soc Chem Commun 11:575–576. https://doi.org/10.1039/C39810000575
50. Osmanova N, Schultze W, Ayoub N (2010) Azaphilones: a class of fungal metabolites with diverse biological activities. Phytochem Rev 9:315–342. https://doi.org/10.1007/s11101-010-9171-3
51. Vasavi HS, Arun AB, Rekha PD (2016) Anti-quorum sensing activity of flavonoid-rich fraction from *Centella asiatica* L. against *Pseudomonas aeruginosa* PAO1. J Microbiol Immunol Infect 49: 8–15. https://doi.org/10.1016/j.jmii.2014.03.012
52. Sarabhai S, Sharma P, Capalash N (2013) Ellagic acid derivatives from *Terminalia chebula* Retz. downregulate the expression of quorum sensing genes to attenuate *Pseudomonas aeruginosa* PAO1 virulence. PLoS one 8:53441. https://doi.org/10.1371/journal.pone.0053441
53. Wang GQ, Li TT, Li ZR, Zhang LC, Zhang LH, Han L, Tang PF (2016, 2016) Effect of negative pressure on proliferation, virulence factor secretion, biofilm formation, and virulence-regulated gene expression of *Pseudomonas aeruginosa* in vitro. Biomed Res Int. https://doi.org/10.1155/2016/7986234
54. Zhou J, Bi S, Chen H, Chen T, Yang R, Li M, Fu Y, Jia AQ (2017) Anti-biofilm and antivirulence activities of metabolites from *Plectosphaerella cucumerina* against *Pseudomonas aeruginosa*. Front Microbiol 8:769. https://doi.org/10.3389/fmicb.2017.00769
55. Musthafa KS, Saroja V, Pandian SK, Ravi AV (2011) Antipathogenic potential of marine *Bacillus* sp. SS4 on N-acyl-homoserine-lactone-mediated virulence factors production in *Pseudomonas aeruginosa* (PAO1). J Biosci 36:55–67. https://doi.org/10.1007/s12038-011-9011-7
56. Das A, Das MC, Sandhu P, Das N, Tribedi P, De UC, Akhter Y, Bhattacharjee S (2017) Antibiofilm activity of *Parkia javanica* against *Pseudomonas aeruginosa*: a study with fruit extract. RSC Adv 7:5497–5513. https://doi.org/10.1039/C6RA24603F
57. Hauser AR (2014) *Pseudomonas aeruginosa* virulence and antimicrobial resistance: two sides of the same coin? Crit Care Med 42. https://doi.org/10.1097/CCM.0b013e3182a120cd
58. Zulianello L, Canard C, Köhler T, Caille D, Lacroix JS, Meda P (2006) Rhamnolipids are virulence factors that promote early infiltration of primary human airway epithelia by *Pseudomonas aeruginosa*. Infect Immun 74:3134–3147. https://doi.org/10.1128/IAI.01772-05
59. Stapper AP, Narasimhan G, Ohman DE, Barakat J, Hentzer M, Molin S, Kharazmi A, Høiby N, Mathee K (2004) Alginate production affects *Pseudomonas aeruginosa* biofilm development and architecture, but is not essential for biofilm formation. J Med Microbiol 53:679–690. https://doi.org/10.1099/jmm.0.45539-0
60. Owlia P, Rasooli I, Saderi H, Aliahmadi M (2007) Retardation of biofilm formation with reduced productivity of alginate as a result of *Pseudomonas aeruginosa* exposure to *Matricaria chamomilla* essential oil. Pharmacogn Mag 3:83
61. Lauridsen RK, Sommer LM, Johansen HK, Rindzevicius T, Molin S, Jelsbak L, Engelsen SB, Boisen A (2017) SERS detection of the biomarker hydrogen cyanide from *Pseudomonas aeruginosa* cultures isolated from cystic fibrosis patients. Sci Rep 7:45264. https://doi.org/10.1038/srep45264

62. Selvamangai G, Bhaskar A (2012) GC–MS analysis of phytocomponents in the methanolic extract of *Eupatorium triplinerve*. Asian Pac J Trop Biomed 2:S1329–S1332. https://doi.org/10.1016/S2221-1691(12)60410-9
63. Kusch P, Deininger S, Specht S, Maniako R, Haubrich S, Pommerening T, Lin PKT, Hoerauf A, Kaiser A (2011) In vitro and in vivo antimalarial activity assays of seeds from *Balanites aegyptiaca*: compounds of the extract show growth inhibition and activity against plasmodial aminopeptidase. J Parasitol Res 2011. https://doi.org/10.1155/2011/368692
64. Padmavathi AR, Abinaya B, Pandian SK (2014) Phenol, 2, 4-bis (1, 1-dimethylethyl) of marine bacterial origin inhibits quorum sensing mediated biofilm formation in the uropathogen *Serratia marcescens*. Biofouling 30:1111–1122. https://doi.org/10.1080/08927014.2014.972386
65. Saxena S, Vineet M, Neha K (2015) *Muscodor tigerii* sp. nov.-volatile antibiotic producing endophytic fungus from the Northeastern Himalayas. Ann Microbiol 65:47–57. https://doi.org/10.1007/s13213-014-0834-y